New SHIVs and Improved Design Strategy for Modeling HIV-1 Transmission, Immunopathogenesis, Prevention and Cure

Hui Li[1*], Shuyi Wang[1*], Fang-Hua Lee[1], Ryan S. Roark[1], Alex I. Murphy[1], Jessica Smith[1], Chengyan Zhao[1], Juliette Rando[1], Neha Chohan[1], Yu Ding[1], Eunlim Kim[1], Emily Lindemuth[1], Katharine J. Bar[1], Ivona Pandrea[2], Cristian Apetrei[3], Brandon F. Keele[4], Jeffrey D. Lifson[4], Mark G. Lewis[5], Thomas N. Denny[6,7], Barton F. Haynes[6,7], Beatrice H. Hahn[1], George M. Shaw[1#]

[1]Departments of Medicine and Microbiology, Perelman School of Medicine, University of Pennsylvania, Philadelphia, Pennsylvania, USA

[2]Department of Pathology, School of Medicine, University of Pittsburgh, Pittsburgh, Pennsylvania, USA

[3]Division of Infectious Diseases, Department of Medicine, School of Medicine, University of Pittsburgh, Pittsburgh, Pennsylvania, USA

[4]AIDS and Cancer Virus Program, Frederick National Laboratory for Cancer Research, Frederick, Maryland, USA

[5]Bioqual, Inc., Rockville, Maryland, USA

[6]Duke Human Vaccine Institute, Duke University School of Medicine, Durham, North Carolina, USA

[7]Department of Medicine, Duke University School of Medicine, Durham, North Carolina, USA

* Hui Li and Shuyi Wang contributed equally. Author order was determined by relative contributions to the conceptual design and conduct of the work presented in the paper.

[#] Corresponding author: George M. Shaw, shawg@pennmedicine.upenn.edu

Abstract

Previously, we showed that substitution of HIV-1 Env residue 375-Ser by bulky aromatic residues enhances binding to rhesus CD4 and enables primary HIV-1 Envs to support efficient replication as simian-human immunodeficiency virus (SHIV) chimeras in rhesus macaques (RMs). Here, we test this design strategy more broadly by constructing SHIVs containing ten primary Envs corresponding to HIV-1 subtypes A, B, C, AE and AG. All ten SHIVs bearing wildtype Env375 residues replicated efficiently in human $CD4^+$ T cells, but only one replicated efficiently in primary rhesus cells. This was a subtype AE SHIV that naturally contained His at Env375. Replacement of wildtype Env375 residues by Trp, Tyr, Phe or His in the other nine SHIVs led to efficient replication in rhesus CD4+ T cells *in vitro* and *in vivo*. Nine SHIVs containing optimized Env375 alleles were grown large-scale in primary rhesus $CD4^+$ T cells to serve as challenge stocks in preclinical prevention trials. These virus stocks were genetically homogeneous, native-like in Env antigenicity and tier-2 neutralization sensitivity, and transmissible by rectal, vaginal, penile, oral or intravenous routes. To facilitate future SHIV constructions, we engineered a simplified second-generation design scheme and validated it in RMs. Overall, our findings demonstrate that SHIVs bearing primary Envs with bulky aromatic substitutions at Env375 consistently replicate in RMs, recapitulating many features of HIV-1 infection in humans. Such SHIVs are efficiently transmitted by mucosal routes common to HIV-1 infection and can be used to test vaccine efficacy in preclinical monkey trials.

64 **Importance**

65 SHIV infection of Indian rhesus macaques is an important animal model for studying
66 HIV-1 transmission, prevention, immunopathogenesis and cure. Such research is timely, given
67 recent progress with active and passive immunization and novel approaches to HIV-1 cure.
68 Given the multifaceted roles of HIV-1 Env in cell tropism and virus entry, and as a target for
69 neutralizing and non-neutralizing antibodies, Envs selected for SHIV construction are of
70 paramount importance. Until recently, it has been impossible to strategically design SHIVs
71 bearing clinically relevant Envs that replicate consistently in monkeys. This changed with the
72 discovery that bulky aromatic substitutions at residue Env375 confer enhanced affinity to
73 rhesus CD4. Here, we show that 10 new SHIVs bearing primary HIV-1 Envs with residue 375
74 substitutions replicated efficiently in RMs and could be transmitted efficiently across rectal,
75 vaginal, penile and oral mucosa. These findings suggest an expanded role for SHIVs as a model
76 of HIV-1 infection.

77

78

Introduction

Simian-human immunodeficiency virus (SHIV) infection of Indian rhesus macaques (RMs) is an important outbred animal model for studying HIV-1 transmission, prevention, immunopathogenesis and cure (1-3). Such research is especially timely, given recent progress with active and passive immunization (4-11) and novel approaches to HIV-1 cure (https://www.niaid.nih.gov/diseases-conditions/hiv-cure-research) (12-18), all of which can benefit from rigorous testing and iterative refinement in animal models. Given the multifaceted roles of HIV-1 envelope (Env) in cell tropism and virus entry, and as a target for neutralizing and non-neutralizing antibodies, the particular features of HIV-1 Envs that are selected for SHIV construction and analysis are of paramount importance. This is especially true for vaccine studies designed to administer (10, 11) or elicit (6, 19, 20) broadly neutralizing antibodies (bNAbs).

SHIVs have a long history dating to 1992 when Sodroski and colleagues first subcloned the *tat*, *rev* and *env* sequences of HIV-1 HXB2c into SIVmac239 (21). This clone was further modified by substitution of the *env* from the dual CCR5/CXCR4 tropic HIV-1 89.6 strain and later adapted by serial passage in RMs, eventually yielding the molecular clone SHIV-KB9 (22). Thus, the earliest SHIVs contained T-cell line adapted, *in vivo* passaged HIV-1 Envs that were CXCR4 tropic, highly syncytium-inducing and cytopathic, and led to accelerated disease in monkeys. As a consequence, many of the essential features of HIV-1 biology, including cell and tissue tropism, sensitivity to neutralizing antibodies (NAbs), immunopathogenesis, transmission efficiency and natural history, were not faithfully represented in the macaque model (3). Attempts to develop a SHIV infection model that included primary (non-T-cell line adapted)

CCR5-tropic Envs were generally met with failure, and when they were successful, such SHIVs often required adaptation by serial monkey passage to achieve consistent replication *in vivo* (3, 23-25). In an attempt to better understand restrictions to SHIV infection and replication in RMs, Overbaugh and Sawyer examined the affinity of primary HIV-1 Envs to rhesus CD4 (26, 27). They discovered that the Envs of most primary HIV-1 strains exhibited low affinity for rhesus CD4 and did not support efficient virus entry into rhesus cells. Overbaugh identified a key amino acid at position 39 in domain 1 of rhesus CD4 that differed between human and rhesus CD4 and was largely responsible for the poor binding and infectivity of primary HIV-1 Envs in rhesus cells (27). This presented a major obstacle to new SHIV designs. Hatziioannou identified a mutation at residue 281 in the CD4 binding region of HIV-1 Env that occurred commonly in SHIV-infected RMs, where it could be shown to facilitate virus replication (28). However, unlike the Env375 substitution, the 281 substitution on its own was unable to consistently convert primary or transmitted/founder (T/F) Envs, which fail to replicate efficiently in RMs, to do so. Moreover, the addition of the 281 mutation to SHIV Envs that already contain a rhesus-preferred Env375 allele, did nothing to further enhance virus replication in rhesus animals (29).

We noted from studies by Finzi and Sodroski (30) that residue 375 in the CD4 binding pocket of primate lentiviral Envs was under strong positive evolutionary pressure across the broad spectrum of primate lentiviruses. These investigators further showed that substitution of 375-Ser (found in most HIV-1 group M viruses) by 375-Trp (found in most SIV strains from lower primates) favored an HIV-1 Env conformation that was closer to the CD4-bound state (31-34). Based on these findings, we hypothesized that residue 375 might act as a “molecular switch” conferring enhanced Env affinity to rhesus CD4 (35) and a lower energetic barrier to

124 conformational change following CD4 binding (31, 34, 36, 37) when the naturally-occurring Ser
125 or Thr residues were substituted by bulky aromatic residues like Trp. In testing this hypothesis,
126 we discovered that substitution of a single residue, 375-Ser, in primary or T/F HIV-1 Envs by Trp,
127 Phe, Tyr, His or Met resulted in SHIVs that exhibited enhanced binding to rhesus CD4, increased
128 infection of primary rhesus $CD4^+$ T cells in culture, and consistent infection and replication by
129 SHIVs in RMs *in vivo* (35). Importantly, these amino acid substitutions at residue 375 did not
130 alter the tier 2 neutralization phenotype of the primary Envs nor did they appreciably alter their
131 sensitivity to bNAbs that targeted any of the canonical bNAb recognition sites, including CD4bs,
132 V2 apex, V3 high mannose patch or membrane proximal external region (35). Thus, it became
133 possible, for the first time, to prospectively design SHIVs that expressed particular primary or
134 T/F Envs, including those that elicited bNAbs in HIV-1 infected humans, and to explore parallels
135 in the immune responses of rhesus monkeys and humans to essentially identical Env
136 immunogens (38). This EnvΔ375 design strategy also made possible the development of SHIVs
137 to evaluate preclinical efficacy of novel active or passive vaccination regimens against challenge
138 by viruses bearing homologous or heterologous primary Envs (7-10). Here, we extend this work
139 by constructing ten new SHIVs, each containing a strategically selected primary HIV-1 Env, that
140 we then validate for retention of native antigenicity, tier 2 neutralization sensitivity and
141 efficient replication in human and rhesus $CD4^+$ T-cells *in vitro* and in RMs *in vivo*. We next
142 describe the development and characterization of a panel of nine SHIV challenge stocks, each
143 containing a unique tier 2 primary HIV-1 Env and grown large scale in primary rhesus $CD4^+$ T-
144 cells, for distribution as challenge strains for active or passive vaccine protection trials. We
145 show that these SHIVs can be efficiently transmitted by different mucosal routes (rectal,

vaginal, penile or oral) and that current vaccination regimens and passively administered bNAbs can prevent transmission of these viruses at neutralization titers similar to those reported in the recently concluded human Antibody-Mediated Prevention (AMP) trials (11). Finally, we describe a new second-generation design strategy that simplifies SHIV construction and eliminates extraneous *tat1* and *env* sequences, thereby making the rhesus-SHIV infection model a more readily accessible and useful research tool.

Results

Ten primary HIV-1 Envs were chosen for SHIV constructions (**Table 1A**). These Envs were selected based on their genetic subtypes, biophysical properties, derivation from primary or T/F virus strains, and in some cases, prior development as candidate vaccine strains for human clinical trials (see **Table 1** for Env features and relevant literature citations). Env subtypes included A, B, C, AE and AG, which complement subtype A, B, C and D SHIVs that we reported previously [see (35, 38); **Table 1B**). All ten of the new SHIVs contained Envs from tier 2 viruses except for Q23.17 Env (39), which has been variably classified as tier 1b or 2 (40-42). Seven of the new SHIVs contained Envs from T/F strains of HIV-1. The 1086 Env (43) corresponds to a vaccine strain employed in the HVTN 703 efficacy vaccine trial (44-46), and the B41 Env was developed as a SOSIP trimer for potential human immunizations (47). The CE1176 Env is from a widely used global test panel for bNAb detection (41). Env RV217.40100 is a new subtype AE T/F strain (48, 49) and Envs CH1012 and CH0694 are T/F strains that elicited potent bNAbs in their respective human hosts (50, 51). Envs T250-4, ZM233, WITO, Q23.17 and CAP256SU were shown previously to bind unmutated common ancestors (UCAs) of human V2 apex targeted bNAbs (52-54). Thus, the Envs selected for new SHIV constructions exhibited unique pedigrees

169 complementary to previous SHIV designs (35, 38, 55-64) that made them desirable for
170 downstream investigations related to HIV-1 transmission, prevention, immunopathogenesis or
171 cure.

172 The design strategy for constructing SHIVs is illustrated in **Fig. 1A.** This construction
173 scheme allowed for the complete extracellular gp140 region of Env plus the transmembrane
174 segment and 9 aa of the cytoplasmic tail (nucleotides 1-2153; HXB2 numbering) to be PCR-
175 amplified *en bloc* and subcloned into a chimeric T/F SIVmac766-HIV-1 proviral backbone (35). If
176 sequences were available for *vpu* in the source material, then the homologous *vpu-env* gp140
177 gene segment was amplified and subcloned into the proviral vector, since homologous *vpu-env*
178 sequences could potentially enhance the efficiency of Env translation. Env 375 codon
179 substitutions corresponding to Trp, Phe, Tyr, His or Met were introduced by site-directed
180 mutagenesis into each SHIV construct, which was then prepared as a large-scale DNA stock and
181 sequence confirmed. Genome sequences for all SHIVs were contributed to GenBank (**Table 1**).
182 For each of the ten primary HIV-1 Envs, six variants containing the different Env375 alleles were
183 made bringing the total number of newly constructed SHIVs to 60. In the course of SHIV
184 constructions, we noted that certain aspects of the design scheme were inefficient, especially
185 the requirement for multiple PCR amplifications and ligations (see Methods). We also found in
186 SHIV infected RMs that redundant *tat1* and *env* gp41 sequences of 68 and 21 bp in length,
187 respectively, that were generated as a consequence of the original cloning strategy underwent
188 spontaneous deletion [**Figs. 1A** and **2**; (35, 38)]. Thus, we modified the SIVmac766 backbone
189 vector and amplification primers to simplify the PCR amplification step and eliminate the
190 redundant sequences (**Fig. 1B**). We used this new design strategy to reclone SHIV.CH505 in

order to perform a head-to-head comparison of viruses expressed from this new vector compared with the original SHIV design, and to clone a new SHIV containing the HIV-1 CH0694 Env. Plasmid DNA for all SHIVs was transfected into 293T cells and virus-containing supernatants were characterized for p27Ag content and infectivity on TZM-bl cells. For all SHIVs, p27Ag concentrations ranged from 200-2000 ng/ml. One nanogram of p27Ag is equivalent to approximately 10^7 virions, so SHIV titers were estimated to range from $2x10^9$ to $2x10^{10}$ virions per ml. We confirmed these titers by quantifying vRNA and assuming two vRNA molecules per virion. Infectivity titers on TZMbl cells ranged from $2x10^5$ to $2x10^6$ per ml, corresponding to an IU to particle ratio of approximately 10^{-4}. This ratio is typical for 293T-derived HIV-1 and SIV virions (35), and 100-fold lower than for virus stocks propagated in primary rhesus $CD4^+$ T cells where between 1 in 100 and 1 in 50 virions are typically infectious on TZMbl cells [**Table 2** and (35)].

For SHIVs bearing the 10 new HIV-1 Envs, we evaluated the replication efficiency of each of them containing six different Env375 residues in primary activated human and rhesus $CD4^+$ T cells *in vitro* (**Fig. 3**). With the exception of SHIV.AE.40100, which naturally contains the positively charged, aromatic residue Env375-His, none of the SHIVs containing wild-type Ser or Thr residues at position Env375 replicated appreciably in rhesus $CD4^+$ T cells (**Fig. 3**). Conversely, all 10 SHIVs with wild-type Env375 residues replicated efficiently in primary activated human $CD4^+$ T cells. This latter result – efficient replication of SHIVs containing wildtype 375 alleles in human $CD4^+$ T cells – was an expected finding but was nonetheless critical to demonstrate, since it confirmed that the chimeric SHIVs that we made were capable of supporting replication. We next asked if substitution of the wildtype Env375 allele by one or

more aliphatic or aromatic residues (Met, Trp, Phe, Tyr or His) would support SHIV replication in rhesus $CD4^+$ T cells. The answer was affirmative for SHIVs expressing each of the ten HIV-1 Envs (**Fig. 3**). The differences in virus replication in rhesus $CD4^+$ T cells between SHIVs expressing wild-type Env375 residues and those expressing bulky aromatic residues was generally quite large, oftentimes resulting in >100-fold differences in p27Ag concentration in culture supernatants at multiple time points throughout the infection (**Fig. 3**). Among the six different Env375 alleles that were tested, Env375-Trp most consistently supported SHIV replication in rhesus $CD4^+$ T cells: it was effective in all 10 HIV-1 Env backbones. Env375-Tyr was the second most favored residue followed by Env375-His or -Phe. It is notable that Trp is also the most conserved Env375 allele across the broad evolutionary spectrum of primate lentiviruses excluding humans and great apes (30). These results thus corroborate and extend a substantial body of scientific literature indicating that SHIVs bearing primary (non-adapted) wildtype HIV-1 Envs rarely replicate efficiently in rhesus cells (1-3, 27-29, 35, 38, 65, 66) and that this restriction can be lifted by substituting a single amino acid at position Env375. In our combined studies [this manuscript plus (35, 38)], we replaced wildtype Env375 residues in 16 primary HIV-1 Envs – 15 of which could not support SHIV replication in RMs – and found in all instances that this substitution alone led to efficient SHIV replication in rhesus animals.

To extend these findings to *in vivo* analyses, we inoculated 41 RMs intravenously in groups of 3 to 6 animals each, with SHIVs containing one of the ten selected HIV-1 Envs and an equal mixture of the six Env375 alleles based on p27Ag content (**Table 3** and **Fig. 4**). We used this experimental design for two reasons: First, because target cell availability is not limited in the initial two weeks of infection during which time virus titers increase exponentially (67-70),

we could use deep sequencing of plasma vRNA/cDNA to directly compare the relative replication rates of the six Env375 allelic variants in an *in vivo* competitive setting. Second, it would be impractical and prohibitively expensive to test 60 SHIVs individually in 60 different monkeys, and even if this could be done, the results would be confounded by monkey-specific variables such as MHC class I and II recognition. Each of the 41 RMs that we inoculated with a SHIV Env375 mixture became productively infected after a single challenge (**Fig. 4**). In most animals, peak viremia occurred at day 14 post-SHIV inoculation and plasma virus load setpoints were reached 16-24 weeks later. Animals treated with anti-CD8 mAb at the time of SHIV inoculation developed significantly higher peak and setpoint viremia titers compared with untreated animals ($p<0.01$ for both). A subset of animals was treated with anti-CD8 mAb at setpoint, 20-50 weeks after infection; most of these animals exhibited increases in virus titers. We performed next generation sequencing (NGS) on plasma samples taken 2 and 4 weeks post-infection to determine the relative replication rates of the different Env375 allelic variants (**Fig. 4**). We expected that differences in infectivity of the Env375 variants would be reflected in the plasma virus quasispecies by two weeks post-inoculation since the combined half-lives of circulating virus and the cells producing it is <1 day (71), resulting in multiple rounds of *de novo* virus infection and replication during this early interval. This was indeed the case. Overall, there was a good correlation between Env375 residues that supported SHIV replication *in vitro* and *in vivo*. For example, in all ten different Env backgrounds, Env375-Ser failed to support SHIV replication in primary rhesus $CD4^+$ T cells *in vitro* (**Fig. 3**) and the same was true in RMs *in vivo* (**Fig. 4**). Conversely, Env375-Trp supported SHIV replication in all ten Env backgrounds *in vitro* and was a predominant allele supporting efficient SHIV replication in 7 of 10 Env backgrounds *in*

257 *vivo*. There were some differences in Env 375 residues that best supported SHIV replication *in*
258 *vitro* versus *in vivo*. For example, for SHIVs bearing ZM233 and CH0694 Envs, 375-Trp supported
259 efficient virus replication *in vitro* but not *in vivo*, where 375-Tyr was dominant. And the Env375-
260 His allele, which is naturally present in most subtype AE viruses including the AE.40100 strain,
261 supported efficient SHIV.AE.40100 replication in rhesus $CD4^+$ T cells *in vitro* but not *in* vivo.
262 Taken together, the findings indicate that substitution of wildtype Env375 alleles in primary
263 HIV-1 Envs with Trp, Tyr or His results in SHIV chimeras that replicate efficiently in RMs.
264 However, since it is impossible to predict with certainty which Env375 allele will best support *in*
265 *vivo* replication of a SHIV bearing any particular HIV-1 Env, an *in vivo* competition experiment
266 similar to that illustrated in **Fig. 4** must be conducted.

267 We also compared the relative replication efficiency of SHIV.CH505.375H generated by
268 the first and second generation construction strategies (**Fig. 5**). We showed previously that in
269 animals infected by viruses produced from the first generation design, that redundant *tat1* and
270 *env* gp41 sequences (68 and 21 bp, respectively) were spontaneously deleted following
271 prolonged *in vivo* replication [**Fig. 2**; (35, 38)]. This suggested a fitness disadvantage for viruses
272 containing the redundant sequences, leading us to hypothesize that animals infected by an
273 equal mixture of the viruses derived from the two designs would show preferential replication
274 by viruses lacking the redundant sequences. This was indeed the case (**Figs. 2A** and **2B**). At
275 three weeks post-infection, viruses lacking the redundant sequences comprised >95% of the
276 plasma virus quasispecies, and by week 8, they comprised >99% of plasma virus.

277 To be a relevant model for HIV-1 vaccine studies, SHIV Envs should exhibit clinically
278 relevant antigenic profiles, neutralization sensitivity phenotypes, and coreceptor usage

indistinguishable from the primary HIV-1 Envs from which they were derived. We evaluated the neutralization sensitivity patterns of Envs expressing the wild-type Env375 allele compared with Envs expressing one or more of the alternative Env375 alleles that were found to support replication in rhesus $CD4^+$ T cells *in vitro* (**Figs. 3**) and in RMs *in vivo* (**Figs. 4**). SHIVs were analyzed using polyclonal anti-HIV-1 sera and a battery of monoclonal antibodies (mAbs) that bind canonical bNAb epitopes, linear V3 epitopes or CD4-induced (CD4i) epitopes (**Fig. 6**). Linear V3 and CD4i epitopes are generally concealed on native Env trimers from primary viruses (40, 72-74), and thus mAbs targeting these epitopes typically fail to neutralize primary virus strains. Conversely, neutralization by linear V3 or CD4i mAbs is generally an indication of a non-native "open" trimer structure typical of laboratory-adapted viruses. In none of the ten primary Env backbones that we tested did Env375 substitutions result in neutralization by linear V3 or CD4i mAbs (**Fig. 6**). Nor did Env375 mutations alter the neutralization sensitivity of these Envs to HIVIG B, HIVIG C or a high titer, broadly neutralizing HIV-1 infected patient plasma specimen CH1754. These results suggest that the Envs bearing residue 375 substitutions retained their native or near-native conformation. These Envs also retained their antigenicity with respect to bNAb epitope presentation since mAbs targeting CD4bs, V2 apex, V3 high mannose patch, and MPER sites exhibited similar neutralization patterns against wild-type and Env375 substituted variants. It is notable that the contours of the neutralization curves, the IC_{50}, IC_{80} and IC_{90} values, and the steep sigmoidal inflections were generally indistinguishable between wildtype Envs and Envs bearing residue 375 substitutions. SHIV.Q23.17 demonstrated neutralization sensitivity patterns to the bNAb mAbs, the three polyclonal anti-HIV IgG and plasma reagents and the mAbs targeting linear V3 or CD4i epitopes that were similar to the other nine SHIVs,

thus supporting a tier 2 status for this virus. We also tested SHIV.CH505.375H derived by first and second generation design schemes for sensitivity to HIV-1 bNAbs, linear V3 targeted mAbs, HIVIG-C and the anti-HIV-1 broadly neutralizing polyclonal plasma CH1754: the two virus preparations showed indistinguishable neutralization sensitivity patterns (**Fig. 5C**). Finally, the SHIVs containing the ten new HIV-1 Envs were tested for coreceptor usage by analyzing their sensitivity to AMD-3100 (a CXCR4 inhibitor) and Maraviroc (a CCR5 inhibitor). Maraviroc, but not AMD-3100, inhibited the entry of all 10 SHIVs in the TZM-bl entry assay (**Fig. 7**), thus demonstrating CCR5-dependent entry. Altogether, the results indicate that Env375 substitutions did not appreciably alter the antigenicity, tier 2 neutralization sensitivity or CCR5 tropism of any of the ten SHIVs.

SHIVs intended for use as challenge strains in preclinical vaccine trials can be generated from 293T cells by transfection of proviral DNA or by virus passage and expansion in primary human or rhesus $CD4^+$ T cells. Each approach has potential advantages and disadvantages (3, 75). We chose to prepare challenge stocks by infecting primary, activated rhesus $CD4^+$ T cells with molecularly cloned virus derived from 293T cell transfections and then expanding the virus as rapidly as possible so as to minimize chances for culture adaptation. By this means, we could ensure that the viral envelopes of challenge stocks contained exclusively rhesus (not human) membrane-associated proteins and that glycosylation patterns would be of rhesus (not human) origin. We selected nine SHIV strains for large scale expansion in rhesus cells and these are listed in **Table 2**. These SHIVs were chosen to be representative of global HIV-1 diversity, including subtypes A, B, C, D, and AG, and to include SHIVs bearing BG505.N332, CH505 and 1086 Envs, which correspond to vaccine candidates in current or recent human clinical trials.

323 Our aim was to generate large numbers of identical replicates of each SHIV stock (>1,000 vials
324 per SHIV), which could then be characterized biophysically for genetic composition, particle
325 content, infectivity, antigenicity and neutralization sensitivity and cryopreserved in vapor phase
326 liquid nitrogen (<160^{o}C) for subsequent distribution to the wider scientific community as
327 validated, standardized SHIV challenge stocks. Thus, we inoculated cultures of 100-200 million
328 primary, activated, rhesus CD4^{+} cells pooled from three naïve Indian RMs at a multiplicity of
329 infection (MOI) of approximately 0.01 with genetically homogeneous, sequence-confirmed,
330 293T transfection-derived virus stocks. For SHIV.CE1176, we infected primary rhesus cells with
331 an equal mixture of Env375-His, Phe and Trp alleles, and for SHIV.T250-4 we infected cells with
332 an equal mixture of Env375-His, Tyr and Trp alleles, because no one of these allelic variants had
333 shown preferential replication in all animals tested (**Fig. 4**). The other SHIV challenge stocks
334 were generated with single Env375 alleles (**Table 2**). On days 7 and 14 post-SHIV inoculation,
335 we added new media and approximately 100-200 million fresh, uninfected rhesus CD4^{+} T cells
336 from three different naïve RMs so as to expand cell numbers and culture volumes while
337 maintaining cell concentrations between 1-2 million per milliliter. Beginning on day ~10 post-
338 SHIV inoculation, we collected the total volume of culture supernatant and replaced it with a
339 greater volume of fresh medium. This complete media collection and replacement was then
340 repeated every 4 days through day 21. By this means, we could collect as much as 2.5 liters of
341 culture medium containing each SHIV over a period of approximately 21 days. Each supernatant
342 collection was centrifuged twice at 2500 rpm (1000g) for 15 minutes to remove any residual
343 cells or cell debris and then immediately frozen in bulk at -80^{o}C. Supernatants were not filtered
344 so as to retain the highest possible infectivity titers. Thus, most of the virus that was collected

and frozen during the 18-21 day culture period was <4 days old and underwent only one freeze-thaw cycle prior to final vialing. After all supernatant collections had been made, they were thawed at room temperature, combined in a sterile 3 liter flask to ensure complete mixing, and then aliquoted into as many as 2,500 cryovials, generally at 1 ml per vial. The vials were then transferred to vapor phase liquid nitrogen for long-term storage. By this means, we could ensure that all vials for any particular SHIV challenge stock were virtually identical in their contents. Between 192 and 2,224 vials per SHIV, each containing between 0.25 and 1.0 ml of challenge stock, were cryopreserved (**Table 2**). Validation analyses were done on thawed cryovial samples to ensure results would be representative of all cryopreserved samples. Challenge stocks were free of bacterial or fungal contamination based on culture on thioglycolate broth. p27Ag concentrations ranged from 73 to 634 ng/ml and vRNA concentrations ranged from 5.0 x 10^8 to 4.1 x 10^9 vRNA /ml. Infectivity was tested on TZM-bl cells where it ranged from 1.5 x 10^5 to 3.2 x 10^7 IU/ml, and on primary rhesus $CD4^+$ T cells where it ranged between 1.9 x 10^3 to 4.1 x 10^6 IU/ml. The genetic composition of the SHIV challenge stocks was analyzed by single genome sequencing of 3' half-genomes to validate the authenticity of each stock and to determine if there was evidence of selection *in vitro* (**Fig. 8A**). Stocks of SHIV.CE1176 and SHIV.T250-4 were sequenced by Illumina deep sequencing to determine the relative proportion of the different Env375 alleles in the final challenge stocks (**Fig. 8B**). Envelope sequence mean and maximum diversity averaged 0.05% (range 0.03-0.13%) and 0.30% (range 0.15-0.42%), respectively in the nine challenge stocks. Mutations across the complete gp160 were essentially random in all challenge stocks except in a secondary expansion of SHIV.CH505. This challenge stock was prepared by infecting naïve rhesus $CD4^+$ T

367 cells with virus from the first expansion of SHIV.CH505 in an attempt to expand sequence
368 diversity and increase infectivity titers. Maximum sequence diversity and maximum sequence
369 divergence from the T/F sequence were 0.35% and 0.29% for stock #2 compared with 0.15%
370 and 0.08%, respectively, for stock #1. p27Ag and vRNA concentrations and infectivity titers on
371 TZMbl cells were similar for stocks #1 and #2 and infectivity titers on primary rhesus CD4 T cells
372 were about 3-fold higher for stock #2 compared with stock #1.

373 HIV-1 strains produced in primary human $CD4^+$ T cells, compared with the same viruses
374 produced in 293T cells, have been reported to exhibit variably greater resistance to neutralizing
375 antibodies (76, 77). These differences have been attributed to differences in Env content, cell
376 adhesion molecules, surface glycan composition or other factors (75). We tested six SHIVs –
377 BG505, CH505, CH848, B41, D.191859 and 1086 – produced in primary rhesus $CD4^+$ T cells and
378 in 293T cells for sensitivity to 17 neutralizing mAbs that targeted CD4bs, V3 glycan, V2 apex,
379 MPER, surface glycan, CD4i or linear V3 epitopes (**Fig. 9**). None of the viruses, regardless of cell
380 derivation, were sensitive to the four mAbs that targeted CD4i or linear V3 epitopes, indicating
381 that they retained a native-like closed Env trimer regardless of the cell of origin. SHIVs
382 produced in 293T cells and primary rhesus cells also exhibited similar overall patterns of
383 sensitivity to the other 15 mAbs in that if a SHIV was sensitive (or resistant) to neutralization by
384 a particular mAb, then this was true regardless of its cell of origin. However, as reported for
385 HIV-1 strains, we observed enhanced resistance to some mAbs by some SHIVs grown in primary
386 rhesus cells compared with 293T cells. This difference was two- to five-fold for all six SHIV
387 strains when exposed to VRC01 and 3BNC117 and as much as 25-fold for certain other virus-

388 antibody combinations such as BG505-CH01, CH505-CH01, CH505-PGT145, CH505-VRC26.25,
389 B41-CH01, B41-VRC26.25, 1086-PGT128 and 1086-VRC26.25 (**Fig. 9**).

390 The properties of rhesus $CD4^+$ T cell grown SHIV challenge stocks summarized in **Table 2**,
391 especially their consistently high virus titers and infectivity measurements, suggested that these
392 virus strains might be suitable for mucosal transmission studies and to assess the preclinical
393 efficacy of actively-induced or passively-administered bNAbs. Nearly all natural routes of HIV-1
394 acquisition result from transmission across mucosal surfaces, the exceptions being intrauterine
395 and intravenous infections. Previously, we showed that SHIVs BG505, CH505 and D.191859 can
396 be transmitted efficiently across rectal, vaginal and oral mucosae (17, 35), resulting in
397 productive clinical infection with virus replication kinetics and plasma virus titers
398 indistinguishable from human infections by HIV-1 (69, 70). Penile acquisition is another
399 important route of HIV-1 transmission in humans (78), and **Fig. 10A** shows that SHIV.D.191859
400 can be transmitted by atraumatic inoculation of foreskin and glans. Peak viremia occurred at
401 approximately 2 weeks post-challenge and plasma virus load setpoint was reached by 6 weeks.
402 Setpoint viremia persisted at 50,000 to 200,000 vRNA molecules per milliliter through 16 weeks
403 of follow-up when the experiment was terminated per protocol. These kinetics of
404 SHIV.D.191859 replication post-penile transmission were similar to plasma virus load kinetics of
405 the same SHIV strain transmitted by intrarectal, intravaginal and intravenous routes (**Fig. 10A**).
406 Lastly, we performed a low-dose, repetitive challenge rectal titration of
407 SHIV.BG505.N332 in 12 naïve RMs to estimate the AID_{50} of the challenge stock and to assess
408 plasma viral load kinetics following IR infection. Three of 4 inoculations at a dose of 1:20 (1 ml),
409 3 of 4 inoculations at a dose of 1:100 (1 ml), and 3 of 9 inoculations at a dose of 1:160 (1 ml)

resulted in productive clinical infection. Acute and early SHIV.BG505.N332 replication kinetics (**Fig. 10B)** were similar to mucosal infection by SHIV.D.191859 (**Fig. 10A**) and also similar to the ten SHIVs illustrated in **Fig. 4** that were infected intravenously. Although our intrarectal AID_{50} titration experiment for SHIV.BG505.N332 involved a small number of animals (n=12) and was subject to stochastic effects related to intrarectal virus inoculation, we could nonetheless estimate the AID_{50} of this stock to be approximately 1:120 (1 ml) for atraumatic IR challenge. This result was corroborated in the control (sham-treated) arm of a preclinical trial assessing the protective efficacy of BG505 SOSIP vaccine elicited neutralizing antibodies against a homologous SHIV.BG505.N332 challenge (7).

Discussion

In recent years, there have been notable advances in HIV prevention and cure research (79-83) yet the goals of effective vaccination and cure – even a "functional" cure – seem far in the distance. Increasingly, experimental medicine trials in humans have been pursued as a strategy to accelerate translational research (82), but at the same time, there remain untapped opportunities and needs for animal models to complement and synergize with human studies to hasten progress. Different scientific questions demand different model systems, ranging from transgenic or humanized mice to outbred small and large animals. Aside from the great apes, which are endangered and thus precluded from laboratory investigation, the rhesus macaque monkey (*Macaca mulatta*) is most similar to humans in its immune repertoire (84, 85). For HIV-related investigations in primates, two classes of viruses are broadly used: simian immunodeficiency viruses (SIV) and chimeric SHIVs that express HIV-1 Envs within an SIV background (3). The present study adds 10 new SHIVs to the research portfolio of HIV

investigators; characterizes key biological properties of these SHIVs that are relevant to virus transmission, prevention, immunopathogenesis and cure research; and describes a new SHIV design strategy and cloning vector that can facilitate future SHIV constructions.

The HIV-1 Env glycoprotein is critical to virus transmission, persistence and pathogenesis since it conveys the essential functions of receptor and coreceptor binding and membrane fusion. At the same time, Env is the target of an array of neutralizing antibodies and cytotoxic T-cells that cause it to evolve continuously in order to escape recognition that would otherwise lead to virus elimination (38, 86, 87). Env accomplishes the latter by means of highly evolved properties, including occlusion of trimer-interface epitopes (88), epitope variation (89), conformational masking (90) and glycan shielding (91). Although HIV-1 Env is notorious for its variability and global diversity (www.hiv.lanl.gov), it is nonetheless constrained in its potential for immediate or near-term evolution due to the myriad of essential biological functions encoded in its sequence (38, 92-94). These constraints can be lifted, however, by prolonged *in vitro* cultivation (66) or extensive passage in unnatural animal hosts (1-3, 22). The implication of these observations is that the most relevant HIV-1 Envs (95) for studies of vaccine-elicited protection, passively acquired antibody protection, or curative intervention are primary or T/F Envs from viruses that are responsible for clinical transmission and the establishment of persistent infection in humans (7-10, 96). T/F Envs express the precise primary, secondary, tertiary and quaternary protein structures that are essential for transmission and T/F Envs are the ones that a vaccine-elicited bNAb response must recognize if it is to be protective (38, 73, 82). Envs derived from short-term virus cultures in human lymphocytes or Env sequences derived from plasma vRNA/cDNA are a first approximation to T/F Envs but they may differ in

important but unrecognized features. Envs derived from extensively passaged virus cultures are less likely to reflect the biologic and antigenic properties of T/F viruses. In this context, 7 of the 10 new SHIVs described in the current study, and 12 of 16 SHIVs that we have reported overall (**Table 1**), were constructed using T/F Envs. The remainder was constructed using primary Envs.

A recent study by Keele and colleagues (29) aimed to create new subtype C T/F SHIVs using 20 South African subtype C T/F Envs and either of two strategies to enhance replication in primary RM $CD4^+$ T cells. One of these strategies was the same EnvΔ375 design employed here and the other was an EnvΔ281 approach reported elsewhere (28). Because the O'Brien study pooled SHIVs for competitive replication analyses in RMs, a precise determination of the proportion of wild-type HIV-1 Envs that could support SHIV replication in monkeys could not be made. However, in the instances where EnvΔ375 substitutions were made and the resulting SHIVs were tested individually, EnvΔ375 substitutions were successful in conferring replication competence to SHIVs in rhesus cells. The addition of EnvΔ281 was neither additive nor synergistic. In our studies described here (**Table 1**) and elsewhere (35, 38), we created a total of 16 EnvΔ375 SHIVs, and each one replicated efficiently in RM CD4+ T cells *in vitro* and in RMs *in vivo*. Altogether, the results suggest that EnvΔ375 substitution is an effective means for creating SHIVs that have a high likelihood of replicating efficiently in RMs. The second-generation design strategy illustrated in **Figs. 1B** and **2** can facilitate this process by substantially reducing the time and effort required to construct new SHIVs and by improving their replication fitness.

A useful outbred primate model for HIV-1 infection of humans should be rational in design, amenable to iterative changes in the challenge viruses, and consistent in reproducing

476 relevant features of disease. Previously, SHIV infections of RMs did not always meet these
477 requirements since SHIVs replicated variably in RMs and often required *in vitro* or *in vivo*
478 adaptations to achieve consistent infection or replication. Oftentimes, these changes were not
479 fully understood mechanistically nor were their immunobiological effects fully appreciated.
480 Moreover, *in vitro* measures of virus content, infectivity and replication in cell culture did not
481 always predict *in vivo* outcomes, lending a measure of uncertainty to SHIV design and analysis.
482 The EnvΔ375 strategy alleviates much of this uncertainty and unpredictability as demonstrated
483 by the following results: i) Env375 substitutions alone were sufficient to enhance Env affinity to
484 rhesus CD4, reduce the energetic threshold for downstream Env transitions following CD4
485 binding, and convey efficient infectivity to the virus in primary rhesus $CD4^+$ T cells *in vitro* and *in*
486 *vivo*; ii) the Env375 substitution strategy worked consistently; every attempt that we (**Table 1**),
487 Keele (29) and Barouch (97) have made to engineer a T/F or primary HIV-1 Env SHIV by residue
488 375 substitution has succeeded in producing a chimeric virus that replicates efficiently in RMs;
489 iii) the ability of such EnvΔ375 SHIVs to replicate *in vivo* was, in each case, predicted by efficient
490 replication in primary, activated rhesus $CD4^+$ T cells *in vitro*; this is a different result from what
491 has been reported for other SHIVs (1-3, 65) and we suspect that our simple EnvΔ375 design
492 scheme, our protocol for rhCD4+ T cell activation, and our method for infecting these cells in
493 tissue culture are responsible for the differences; iv) the antigenicity and tier 2 neutralization
494 sensitivity of wildtype HIV-1 Envs was closely mirrored by EnvΔ375 mutants expressed from
495 293T cells or as infectious SHIVs from primary rhesus CD4 T cells; v) the genetic diversity of each
496 SHIV infection stock was very low when virus was expressed either from 293T cells or from
497 primary rhesus $CD4^+$ T-cells; vi) transmission efficiency of SHIVs across rhesus rectal, vaginal,

498 penile and oral mucosa, and intravenously, mirrored the transmission efficiency of HIV-1 in
499 humans; vii) acute and early SHIV replication dynamics in RMs measured by plasma vRNA
500 replicated what has been seen in humans, including a 7-14 day eclipse period before vRNA is
501 detectable in plasma, an exponential increase in plasma virus load to a peak approximately 14-
502 28 days post-infection, establishment of setpoint viremia two or more months later, and
503 immunopathogenesis leading to clinically-defined AIDS in a subset of animals (69, 70, 73); viii)
504 SHIV infected RMs consistently elicited autologous, strain-specific NAbs, and in some cases
505 bNAbs, with kinetics similar to HIV-1 infected humans (35, 38); ix) molecular pathways of SHIV
506 Env evolution in RMs closely mirrored evolution of homologous HIV-1 Envs in humans, including
507 precise molecular patterns of Env-Ab coevolution leading to Nab escape, and in some animals,
508 the development of bNAbs (38). The latter results speak to the native-like structure of SHIV
509 Envs and to homologies and orthologies in human and rhesus immunoglobulin gene repertoires
510 (38, 85). Altogether, the findings highlight the reproducibility and relevance of the SHIV
511 EnvΔ375 infected RM as a model system for HIV-1 infection in humans. There are, however,
512 limitations to the SHIV EnvΔ375 infected RM as a model for cure studies, since persistent virus
513 replication is variable between different SHIVs and even with the same SHIV in different
514 animals [**Fig. 4** and (35, 38)]. SHIVs D.191859, BG505.N332 and CH505 have generally shown
515 the most consistent replication across multiple studies in monkeys that were not treated with
516 anti-CD8 mAb; replication of these and other SHIVs was generally enhanced by about 10-fold by
517 the administration of rhesus anti-CD8 mAb at the time of SHIV inoculation (**Fig. 4**). On the other
518 hand, a mechanistic understanding of the basis of spontaneous control of SHIV replication in

some monkeys but not others could conceivably inform studies of functional HIV-1 cure in humans.

Efficient mucosal transmission leading to productive clinical infection with consistent patterns of plasma viremia are critical features of SHIVs intended for use as challenge strains to test for vaccine efficacy and for mechanistic studies of virus transmission. We tested SHIVs BG505.N332, CH505, D.191859 and T250-4 for mucosal transmission and titered each challenge stock for 50% animal infectious doses (AID_{50}). For these studies, virus challenge stocks were grown in primary rhesus $CD4^+$ T cells. Challenge stocks were first subjected to thorough analytical measurements of virus concentration, infectivity, genotypic complexity and phenotype with respect to coreceptor usage and antigenicity (**Table 2** and **Figs. 7-9**). Because of the wide scientific interest of BG505.N332 SOSIP as a vaccine candidate, we conducted a low-dose atraumatic intrarectal titration study of SHIV.BG505.N332 (**Fig. 10B**) where we estimated the IR AID_{50} of this stock to be approximately 1:120 (1 ml). Burton and colleagues (7) corroborated this estimate by showing that 6 of 6 naïve RMs inoculated intrarectally with a 1:20 (1 ml) dose of this same challenge stock, and 9 of 12 naïve RMs inoculated intrarectally with a 1:75 (1 ml) dose, became productively infected after a single challenge (7). Importantly, these results demonstrated reproducibility in clinical infectivity titers of the identical challenge stock used at different primate centers and in animals obtained from different breeding colonies. Replication dynamics of SHIV.BG505.N332 following the low dose intrarectal inoculations were quite similar in the two studies [**Fib. 10B** and (7)]: a meta-analysis of the results revealed peak viremia geometric mean titers of 2.7×10^6 vRNA/ml at day 14 post-challenge and plasma viral load setpoint geometric mean titers of 9.2×10^3 vRNA/ml by week 12, with 23 of 24 animals

541 remaining viremic. Pulendran and colleagues used this same SHIV.BG505.N332 challenge stock
542 for low dose intravaginal challenges in a preclinical protection study in RMs (9). In a control arm
543 of 15 sham vaccinated RMs, they found the AID_{50} to be approximately 1:3 (1 ml). Peak plasma
544 viremia (GMT = 1.7 x 10^6 vRNA/ml) was again at 14 days post-infection and plasma viral load
545 setpoint was reached by week 10, with 14 of 15 animals remaining viremic (GMT = 1.7 x 10^3
546 vRNA/ml). The 40-fold difference in AID_{50} between IR and IVAG challenge routes is consistent
547 with previous findings with SHIV and SIVs (3, 98, 99) and is similar to estimates of relative
548 infectivity in humans exposed to receptive anal intercourse versus receptive vaginal intercourse
549 (78). We also titrated SHIV.CH505 challenge stocks for AID_{50} in RMs following intrarectal or
550 intravaginal inoculation. In independent studies with a total of 21 RMs, Klatt [(100) and
551 unpublished data] and Haynes estimated the AID_{50} following IR challenge of naïve RMs to be
552 approximately 1:80 (1 ml), while Felber and colleagues (8) found the AID_{50} of this stock
553 following IVAG challenge to be approximately 1:2 (1 ml) (**Table 2)**. These findings again
554 demonstrate reproducibility in AID_{50} titers in different primate centers and in monkeys from
555 different breeding colonies as well as a 30-40 fold difference in infectivity between IR versus
556 IVAG challenge routes. Previously, we estimated the AID_{50} for SHIV.D.191879 for IVAG
557 inoculation to be approximately 1:3 (1 ml) (101). Here, we could not estimate an AID_{50} for
558 penile transmission by the SHIV.D.191879 challenge stock since 2 of 2 animals became infected
559 after a single inoculation (**Fig. 10A**), but the findings suggest that the AID_{50} titers of this stock
560 for penile transmission are likely to be sufficient for it to be used as a challenge stock in
561 preclinical prevention trials once formal titering is completed. Finally, in an ongoing study, Sok,
562 Rakasz and colleagues have estimated the AID_{50} of SHIV.T250-4 to be approximately 1:160 (1 ml

563 inoculum) following atraumatic rectal inoculation (unpublished). Thus, in multiple studies of
564 mucosal infection by BG505.N332, CH505, D.191859 and T250-4, AID_{50} titers and post-infection
565 plasma viral load kinetics were consistent between SHIVs and between studies conducted at
566 different primate facilities and mirrored analytical assessments of the different challenge stocks
567 *in vitro* (**Table 2)**. These findings suggest that precise measurements of virion content and
568 infectivity of different challenge stocks correlate well with AID_{50} titers following mucosal
569 challenge, which is important because it can facilitate AID_{50} titrations of new challenge stocks
570 going forward.

571 Altogether, the findings of this study suggest that the SHIVs listed in **Table 1** can be
572 broadly useful as challenge stocks for preclinical studies of vaccine-elicited or passively-
573 acquired antibody protection; for assessing novel cure interventions; and for mechanistic
574 studies of virus transmission and pathogenesis. We have contributed the rhCD4 T cell grown
575 SHIV challenge stocks and the 16 SHIV plasmid DNA stocks to the NIH NIAID HIV Reagent
576 Repository and to the Penn Center for AIDS Research Virology Core Laboratory, which provides
577 investigators with derivative reagents (e.g., barcoded SHIVs for lineage-tracing, sequence-
578 verified viral DNA maxipreps, minimally-adapted T/F SHIV variants with enhanced *in vivo*
579 replication dynamics, and titered 293T derived infectious virus stocks) to meet research needs.
580 One important research application that we anticipate in the future is in comparative efficacy
581 testing of different vaccines against common heterologous tier 2 primary virus challenge stocks,
582 and the same vaccine against a common heterologous virus administered by different mucosal
583 inoculation routes. Such studies promise to inform HIV-1 immunogen design and testing as new
584 vaccine candidates are developed.

585

586

587 **Materials and Methods**

588 **Ethical Statement.** Indian rhesus macaques were housed and studied at Bioqual, Inc., Rockville,
589 MD or at the Plum Borough animal facility at the University of Pittsburgh, Pittsburgh, PA,
590 according to guidelines and standards of the Association for Assessment and Accreditation of
591 Laboratory Animal Care and the Animal Welfare Act. Experiments were approved by the
592 Bioqual, University of Pittsburgh, Duke University and University of Pennsylvania Institutional
593 Animal Care and Use Committees. All RMs included in this study were socially housed (paired)
594 indoors in stainless steel cages, had 12/12 light cycle, were fed twice daily, and water was
595 provided *ad libitum*. A variety of recommended environmental enrichment strategies were
596 employed. The animals were observed twice daily and any signs of disease or discomfort were
597 reported to the veterinary staff for evaluation. For sample collections, animals were
598 anesthetized with 10mg/kg ketamine HCl (Park-Davis, Morris Plains, NJ, USA) or 0.7 mg/kg
599 tiletamine (HCl) and zolazepan (Telazol, Fort Dodge Animal Health, Fort Dodge, IA) injected
600 intramuscularly. At the end of the study, the animals were sacrificed by intravenous
601 administration of barbiturates.

602 **Nonhuman primate care and procedures.** Animals were approximately equally divided male
603 and female, aged 3-12 years and negative for Mamu-A*01, B*08, and B*17. Animals were
604 screened to be negative for retroviruses, measles, ebola and *T. cruzi*. Animals were sedated for
605 blood draws, anti-CD8 mAb infusions, and SHIV inoculations. For estimations of AID_{50} of SHIV
606 challenge stocks, animals were inoculated atraumatically by penile, rectal or vaginal routes.
607 Penile inoculations were performed in anesthetized animals in a recumbent supine position.

608 The foreskin was retracted vertically and laterally and separated from the glans exposing the
609 preputial mucosa and coronal sulcus. 0.25 ml of undiluted SHIV challenge stock was slowly and
610 carefully inoculated into this potential space using a 1 ml syringe and the vertical-lateral
611 foreskin retraction maintained for 20 minutes. Intrarectal or intravaginal inoculations were
612 performed by inserting a flexible lubricated pediatric feeding tube atraumatically 3-5 cm into
613 the rectum or vagina of animals lying in a Trendelenburg position followed by the
614 administration of diluted virus stock in a total volume of 1 ml by slow push. Animals were
615 maintained in Trendelenburg position for 30 minutes before being repositioned and returned
616 to their cages to recover from anesthesia. Intravenous SHIV inoculations were performed by
617 placing an intravenous catheter into the femoral vein of anesthetized animals in supine
618 position, administering small volumes of sterile normal saline and confirming venous access by
619 retrograde blood return. SHIVs bearing any of 10 different HIV-1 Envs, each with as many as six
620 Env375 allelic variants in a total volume of 1 ml DMEM medium, were administered by slow
621 push. The different Env375 allelic variants were equilibrated based on p27Ag concentration,
622 since the variable we were testing was relative infectivity as reflected in SHIV replication
623 efficiency and plasma vRNA load *in vivo*. Thus, a typical inoculum consisted of a total of 300 ng
624 SHIV p27Ag, comprised of 50 ng p27Ag of each of six SHIV Env375 variants. Following virus
625 inoculation, the IV line was flushed with normal saline. A subset of animals then received an
626 intravenous infusion of 25 mg/kg of anti-CD8alpha mAb [MT807R1; NIH Nonhuman Primate
627 Reagent Resource, NHPRR (https://www.nhpreagents.org/)] or anti-CD8beta mAb
628 (CD8beta255R1; NHPRR) mAb over a period of 3-5 minutes. Another subset of animals received

anti-CD8 mAb at 18-48 weeks post infection. RMs were phlebotomized weekly, then monthly, and then every other month to collect and cryopreserve blood samples.

Processing and storage of rhesus and human blood specimens. Blood samples from rhesus macaques were collected in sterile 10 ml vacutainers containing ACD-A anticoagulant. Up to 40 ml of ACD-A anticoagulated blood from each RM was combined in a sterile 50 mL polypropylene conical tube, centrifuged at 2100 rpm (1000xg) for 10 min at 20^{o}C, and the plasma collected in a fresh 50 mL conical tube without disturbing the buffy coat WBC layer and large red cell pellet. The plasma was centrifuged again at 3,000 rpm (~2000xg) for 15 minutes at 20^{o}C in order to remove all platelets and cells. Plasma was collected and aliquoted into cryovials and stored at -80^{o}C. The RBC/WBC pellet was resuspended in an equal volume of Hanks balanced salt solution (HBSS) without Ca^{++} or Mg^{++} and containing 2mM EDTA and then divided into four 50 ml conical tubes. Additional HBSS-EDTA (2mM) buffer was added to bring the volume of the RBC/WBC mixture to 30 ml in each tube. The cell suspension was then carefully underlayered with 14 ml 96% Ficoll-Paque and centrifuged at 1800 rpm (725xg) for 20 min at 20^{o}C in a swinging bucket tabletop centrifuge with slow acceleration and braking so as not to disrupt the ficoll-cell interface. Mononuclear cells at the ficoll interface were collected and transferred to a new 50ml centrifuge tube containing HBSS-EDTA (w/o Ca^{++} or Mg^{++}) and centrifuged at 1000 rpm (~200 g) for 15 min at 20^{o}C. This pellets PBMCs and leaves most of the platelets in the supernatant. The supernatant was removed and the cell pellet was resuspended in 40 ml HBSS (with Mg^{++}/Ca^{++} and without EDTA) + 1% FBS. To remove additional contaminating platelets, the cell suspension was centrifuged again at 1000 rpm (~200xg) for 15 minutes at 20^{o}C and the supernatant discarded. The cell pellet was tap-resuspended in the

651 residual 0.1-0.3 ml of media and then brought to a volume of 10 ml HBSS (with Mg^{++}/Ca^{++}) plus
652 1% FBS. Cells were counted and viability assessed by trypan blue exclusion. Cells were
653 centrifuged again at 1200rpm (300xg) for 10 min at 20°C, the supernatant discarded, and the
654 cells resuspended at a concentration of 5-10x10^6 cells/ml in CryoStor cell cryopreservation
655 media (Sigma Cat. C2999), aliquoted into 1ml cryovials (CryoClear cryovials; Globe Scientific
656 Inc., Cat. 3010), placed in a Corning CoolCell LX cell freezing container, stored overnite at -80°C,
657 and then transferred to vapor phase liquid N_2 for long-term storage. Alternatively, freshly
658 isolated rhesus PBMCs were processed immediately for $CD4^+$ T cell purification and activation.
659 Human PBMCs from de-identified normal blood samples were isolated by similar procedures
660 from leukopaks obtained from the University of Pennsylvania Comprehensive Cancer Center
661 Human Immunology Core Laboratory and either cryopreserved or used immediately for $CD4^+$ T
662 cell purification and activation.

663 **SHIV constructions.** SHIVs were constructed in one of two chimeric SIV/HIV proviral backbone
664 plasmids. The original backbone (**Fig. 1A**) was first described by Li et al. (35) and was used in
665 that study to generate SHIV.A.BG505, SHIV.B.YU2, SHIV.C.CH505, SHIV.C.CH848 and
666 SHIV.D.191859. This backbone was subsequently employed by Roark to generate
667 SHIV.C.CAP256SU (38) and by other investigators to generate still other SHIVs, all based on this
668 EnvΔ375 design strategy (29, 97). We designated the first generation plasmid as
669 pCRXTOPO.SHIV.v1.backbone1 and pCRXTOPO.SHIV.v1.backbone2. Version 1 backbones 1 and
670 2 allow for the cloning of *vpu-env* (*env* nucleotides 1-2153, HXB2 numbering) or *env*-only (*env*
671 nucleotides 1-2153, HXB2 numbering) amplicons, respectively. This first generation plasmid
672 required cumbersome sequential PCR amplifications and ligations in order to generate a

673 complete replication competent chimeric SHIV provirus. In addition, the first generation design
674 scheme generated an SIV – HIV-1 *tat1* redundancy and an HIV-1 *env* gp41 redundancy, both of
675 which were spontaneously deleted when SHIVs replicated persistently *in vivo* [e.g., see **Fig. 2A**
676 and (35, 38)]. We thus engineered second generation SHIV cloning vectors designated
677 pCRXTOPO.SHIV.v2.backbone1 and pCRXTOPO.SHIV.v2.backbone2, which allow for cloning of
678 the identical *vpu-env* and *env*-only amplicons, respectively. In the first generation SHIV
679 backbone, unique restriction enzyme recognition sites for *BstBI* and *XhoI* are present in the
680 middle of SIV vpx and after the 3' LTR in the vector sequence, respectively. We synthesized two
681 fragments that contain these two enzyme sites and the genes in between. We eliminated the
682 redundant *tat1* and *env* gp41 sequences and replaced the *vpu-env* and *env* genes with a linker
683 fragment that carries two *BsmBI* restriction enzyme sites (**Fig. 1**). The *BsmBI* site appended at
684 the N-terminus of the linker recognizes the reverse complementary DNA strand and creates a 3'
685 overhang; the one added at the C-terminus recognizes the positive strand DNA and creates a 5'
686 overhang. This design results in two different sticky ends, which allows unidirectional cloning of
687 the insert into the backbone. *BsmBI* is a Type IIS restriction enzyme that cleaves outside of its
688 recognition site and thus the enzyme recognition sequence does not remain after ligating the
689 insert into the backbone (**Fig. 1**). The two synthesized fragments were then cloned into the
690 original SHIV backbone separately using the BstBI and XhoI sites. The resulting two SHIV
691 backbones (GenBank accession nos. MW476487 and MW476488) were then used for cloning
692 *env* (nucleotides 1-2153, HXB2 numbering) or *vpu-env*, respectively. The *vpu-env* gp140
693 segments of HIV-1 CE1176, CH1012, T250-4, Q23.17, WITO, ZM233, 1086, B41 and 40100 were
694 cloned into the first generation SHIV backbone using methods described previously (Li, et al.,

695 2016). The *vpu-env* gp140 segments of HIV-1 CH0694 and CH505 were cloned into the second
696 generation SHIV backbone by appending the *BsmBI* recognition sequences to 5' and 3' ends of
697 the amplicon and performing a standard ligation (35). We then used the QuikChange II XL Site-
698 Directed Mutagenesis kit (Agilent Technologies) to create allelic variants (M, Y, F, W, or H) of
699 the wild type Env375-Ser or -Thr codons. Wild type and mutant plasmids were transformed into
700 MAX Efficiency Stbl2 Competent Cells (Invitrogen) for maxi-DNA preparations. Each 10-kb viral
701 genome was sequenced in its entirety to authenticate its identity and genome integrity.
702 Infectious SHIV stocks were generated in 293T cells as previously described.

703 **SHIV Infection of primary rhesus and human CD4$^+$ T cells.** Purified rhesus and human CD4$^+$ T
704 cells were isolated from PBMCs using magnetic MACS CD4 MicroBeads (Miltenyi Biotec), as
705 previously described (35). They were activated by incubation with anti-biotin MACSiBead
706 particles (Miltenyi Biotec) loaded with biotinylated anti-CD2, -CD28 and -CD3 mAbs, as
707 previously described (35). The replication kinetics of each of the SHIVs and Env375 variants in
708 primary, activated human and rhesus CD4$^+$ T cells were determined again as previously
709 described (35). Briefly, 293T supernatants containing 300 ng p27Ag of each variant, were
710 added to 2 x 10^6 purified human or rhesus CD4 T cells in complete RPMI growth medium
711 (RPMI1640 with 15% heat-inactivated fetal bovine serum (FBS, Hyclone), 100 U/mL penicillin–
712 streptomycin (Gibco), 30 U/mL IL-2 (aldesleukin, Prometheus Laboratories) and 30 µg/ml DEAE-
713 Dextran. 300 ng p27Ag is equal to ~3 x 10^9 virions, ~3 x 10^5 IU on TZMbl cells, or ~3 x 10^4 IU on
714 primary CD4$^+$ T-cells, so the estimated MOI of this titration was estimated to be between 0.01
715 and 0.05. The cell and virus mixtures were incubated for 2 hours under constant rotation at
716 37^{o}C to facilitate infection, washed three times with RPMI1640, and resuspended in complete

717 RPMI1640 medium lacking DEAE-Dextran. Cells were plated into 24-well plates at 2 million cells
718 in 1 ml and cultured for 13 days, with sampling of 0.2ml supernatant and media replacement
719 every 2-3 days. Supernatants were assayed for p27Ag concentration by ELISA according to
720 manufacturer's instructions (Zeptometrix).

721 **SHIV challenge stock generation in primary rhesus CD4$^+$ T cells.** 100-200 million primary,
722 activated, rhesus CD4$^+$ cells pooled from three naïve RMs at a concentration of 10^7 cells/ml in
723 complete RPMI1640 medium with 10% FCS and DEAE-Dextran (30 ug/ml) were inoculated with
724 293T cell-derived SHIVs at a MOI of 0.1-0.5 in TZM-bl cells and an estimated MOI of 0.01-0.05 in
725 primary rhesus CD4$^+$ T cells. For SHIV.CE1176, we infected primary rhesus cells with an equal
726 mixture of Env375-His, Phe and Trp alleles, and for SHIV.T250-4 we infected cells with an equal
727 mixture of Env375-His, Tyr and Trp alleles, because these alleles in these two Env backgrounds
728 had shown differential replication in different animals (**Fig. 3**). The other SHIV challenge stocks
729 were generated with viruses containing single rhesus-preferred Env375 alleles (**Table 2**). Total
730 volume of the SHIV-cell mixture was typically 10-30 ml, depending of the infectivity titers of the
731 293T virus stock. The SHIV-cell mixture was transferred to a T75 flask, which was fixed to a
732 rotating wheel or rocker so that leakage or spillage was not possible. This apparatus was then
733 placed in a 37^{o}C 5% CO_2 incubator for 2 hours of continuous mixing. The contents of the T75
734 flask were then transferred to a sterile 50 ml polypropylene tube and centrifuged at room temp
735 at 1200 rpm (~300xg) for 10 min. Supernatant was decanted, the cells gently tap resuspended
736 in the residual medium (<0.5 ml) and then resuspended in 50 ml complete RPMI medium with
737 10% FCS and the wash step repeated twice. The washing steps are important to remove DEAE-
738 dextran, which can be toxic to cells in culture, and to remove unbound virus. Cells were then

739 resuspended at a concentration of 1-2x10^6 cells/ml in complete RPMI1640 medium with 10%
740 FCS, Il-2 and antibiotics in T100 flasks and incubated at 37^{o}C in a 5% CO_2 incubator. On days ~7
741 and ~14 post-SHIV inoculation, additional fresh media and approximately 100-200 million
742 fresh, uninfected, activated rhesus $CD4^+$ T cells from three different naïve RMs were added to
743 the cultures, which were transferred into T250 flasks to accommodate larger volumes. This
744 expansion of the cultures markedly increased cell numbers and supernatant volumes while
745 maintaining cell concentrations between 2-4 million per milliliter. The culture supernatant was
746 sampled on approximately days 1, 4, 7, 10, 14, 17 and 20 for p27Ag concentration with assays
747 performed weekly. Typically, p27Ag concentrations were <50 ng/ml on day 7 but rose rapidly to
748 >200 ng/ml by day 10. On day ~10 post-SHIV inoculation, the total volume of culture
749 supernatant was collected, centrifuged twice at 2500 rpm (1000xg) for 15 minutes to remove
750 any residual cells or cell debris, and then frozen in bulk at -80^{o}C. The supernatant was replaced
751 with a greater volume of fresh medium as additional uninfected activated rhesus $CD4^+$ T cells
752 were added and as cells divided, again keeping cell concentrations a 2-4 million per milliliter.
753 Between days 10 and 21, p27Ag production was maximal and concentrations in the
754 supernatant rose rapidly to >200 ng/ml every 3-4 days after each complete collection of culture
755 supernatant. By this means, we could collect as much as 2.5 liters of culture medium containing
756 each SHIV over a three week culture period. Importantly, because complete supernatant
757 collections and fresh media replacements were performed every 3-4 days beginning on day
758 ~10 post-SHIV inoculation, most of the virus that was collected and frozen was <4 days old and
759 underwent only one freeze-thaw cycle prior to final vialing. Once all supernatant collections
760 had been made over the 18-21 day culture period, they were thawed at room temperature at

the same time, combined in a sterile 3 liter flask to ensure complete mixing, and aliquoted into as many as 2,500 cryovials, generally at 1 ml per vial. The vials were then transferred to a -80°C freezer overnight and then to vapor phase liquid nitrogen for long-term storage. By this means, we could ensure that all vials were essentially identical in their contents.

Virus entry and neutralizing antibody assays. Assays for virus entry and neutralizing antibodies were performed using TZM-bl indicator cells, as previously described (35, 91). The NAb assay is essentially identical to that employed by Montefiori, Seaman and colleagues (102) (https://www.hiv.lanl.gov/content/nab-reference-strains/html/home.htm), the only difference being that we plate virus and test plasma or mAbs or purified polyclonal IgG onto adherent TZM-bl cells and hold the concentration of human and rhesus plasma/serum constant across all wells at 10%. In addition to this 10% final concentration of plasma/serum, the culture medium consists of Dulbecco's Modified Eagle's Medium (DMEM) with 40 μgm/ml of DEAE-dextran and pen/strep antibiotics. Infections were performed in duplicate. Uninfected cells were used to correct for background luciferase activity. The infectivity of each virus without antibodies was set at 100%. The 50% inhibitory concentration (IC_{50}) is the antibody concentration that reduces by 50% the RLU compared with the no Ab control wells after correction for background. Nonlinear regression curves were determined and IC_{50} values calculated by using variable slope (four parameters) function in Prism software (v8.0). In the virus entry assay used to determine infectivity titers of 293T cell-derived viruses (**Table 2**), the culture medium consists of DMEM with 10% FBS, 40 μgm/ml DEAE dextran and pen/strep antibiotics and cell entry is quantified by beta-galactosidase expression after 48 hours, as described (35).

782 **Coreceptor use analysis.** TZM-bl cells were seeded in 96-well plate at density of 15,000 cells per
783 well and cultured overnight at 37°C with humidified air and 5% CO_2. Cells were incubated with
784 selective entry inhibitors for 1 hour, followed by inoculation of 2,000 TZMbl IU of virus per well.
785 Coreceptor inhibitors included 10 µM Maraviroc (CCR5), 1.2 µM AMD3100 (CXCR4), a mixture
786 of inhibitors or media control. Viral Envs YU2 (CCR5-tropic) and SG3 (CXCR4-tropic) were
787 included as controls. The infectivity of the media control wells was set at 100%. The infectivity
788 of the experimental wells was quantified by percent of infection compared with the media
789 control wells after correction for background.
790 **Plasma viral RNA quantification.** Plasma viral load measurements were performed by the AIDS
791 and Cancer Virus Program, Leidos Biomedical Research Inc., Frederick National Laboratory and
792 by the NIH/NIAID-sponsored Nonhuman Primate Virology Core Laboratory at the Duke Human
793 Vaccine Institute, as previously described (35, 38). Over the course of this study, the sensitivity
794 limits for accurate vRNA quantification using 0.5 ml of NHP plasma improved from 250 RNA
795 cp/ml to <100 RNA cp/mL. We chose a conservative threshold of 100 RNA cp/mL for a limit of
796 detection and 250 RNA cp/mL for the limit of quantification.
797 **Viral RNA Sequencing.** Single genome sequencing of SHIV 3' half genomes was performed as
798 previously described (35, 73). Geneious software was used for alignments and sequence
799 analysis. The sequences were visualized using the LANL Highlighter plot tools
800 (https://www.hiv.lanl.gov/content/sequence/HIGHLIGHT/highlighter_top.html). To analyze the
801 prevalence of 375 variants, next-generation sequencing was performed using Illumina MiSeq
802 system as described (35, 38). For each animal, 20,000-200,000 vRNA copies were used for
803 reverse transcription and bulk RT-PCR. Raw reads from each bulk PCR were analyzed and the

804 frequency of S, T, M, Y, H, W, and F codons at position 375 was determined by using Geneious
805 software.

806 **Statistical analyses.** Statistical tests were calculated by using GraphPad Prism 8 software. The
807 Mann-Whitney test was used to determine whether the peak and setpoint viral loads of anti-
808 CD8 treated animals were significantly different from untreated animals. We chose a
809 nonparametric rank-based test because both peak and setpoint viral loads of the untreated
810 group failed the D'Agostino & Pearson normality test (P-values < 0.05). The geometric means
811 were calculated using the Column statistics function of GraphPad Prism 8. The mean and
812 maximum diversities were calculated using Poisson-Fitter v2 program
813 (https://www.hiv.lanl.gov).

814 **Data availability.** Sequences determined in the present study are available in GenBank under
815 accession numbers KU958487, MW410732 to MW410742, MW476487 and MW476488,
816 MW484951 to MW484987, and MW507842 to MW508333.

817

818

819

820 **Acknowledgments**

821 We thank the staff at Bioqual, Inc., for exceptional care and assistance with experiments
822 involving nonhuman primates, and T. Demarco, N. DeNaeyer and members of the Nonhuman
823 Primate Virology Core Laboratory at the Duke Human Vaccine Institute for SHIV plasma vRNA
824 measurements. We thank N. Miller, J. Warren, Q. Dang and S. Staprans for helpful discussions
825 regarding the development of SHIVs as a research community resource.

826 This work was funded by the Bill & Melinda Gates Foundation (OPP1145046, OPP1206647/INV-
827 007939) and the Division of AIDS (NIAID/NIH) through support of the Duke Center for HIV/AIDS
828 Vaccine Immunology-Immunogen Discovery (UM1 AI100645) and Consortium for HIV/AIDS
829 Vaccine Development (UM1 AI144371), the Penn Center for AIDS Research (P30 AI045008), and
830 grants AI088564, AI094604, AI131251, AI131331, AI050529, and AI150590. R. Roark was
831 supported by an NIH training grant in HIV Pathogenesis (T32-AI007632). This project has been
832 funded in part with Federal funds from the National Cancer Institute, National Institutes of
833 Health, under Contract No. HHSN261200800001E and 75N91019D00024. The content of this
834 publication does not necessarily reflect the views or policies of the Department of Health and
835 Human Services, nor does mention of trade names, commercial products, or organizations
836 imply endorsement by the U.S. Government.
837

838 **References**
839
840 1. Hatziioannou T, Evans DT. 2012. Animal models for HIV/AIDS research. Nat Rev
841 Microbiol 10:852-67. https://doi.org/10.1038/nrmicro2911.

842 2. Sharma A, Boyd DF, Overbaugh J. 2015. Development of SHIVs with circulating,
843 transmitted HIV-1 variants. J Med Primatol 44:296-300.
844 https://doi.org/10.1111/jmp.12179.

845 3. Del Prete GQ, Lifson JD, Keele BF. 2016. Nonhuman primate models for the evaluation
846 of HIV-1 preventive vaccine strategies: model parameter considerations and
847 consequences. Curr Opin HIV AIDS 11:546-554.
848 https://doi.org/10.1097/COH.0000000000000311.

849 4. Hessell AJ, Poignard P, Hunter M, Hangartner L, Tehrani DM, Bleeker WK, Parren PW,
850 Marx PA, Burton DR. 2009. Effective, low-titer antibody protection against low-dose
851 repeated mucosal SHIV challenge in macaques. Nat Med 15:951-4.
852 https://doi.org/10.1038/nm.1974.

853 5. Hessell AJ, Malherbe DC, Haigwood NL. 2018. Passive and active antibody studies in
854 primates to inform HIV vaccines. Expert Rev Vaccines 17:127-144.
855 https://doi.org/10.1080/14760584.2018.1425619.

856 6. Pauthner M, Havenar-Daughton C, Sok D, Nkolola JP, Bastidas R, Boopathy AV,
857 Carnathan DG, Chandrashekar A, Cirelli KM, Cottrell CA, Eroshkin AM, Guenaga J,
858 Kaushik K, Kulp DW, Liu J, McCoy LE, Oom AL, Ozorowski G, Post KW, Sharma SK,
859 Steichen JM, de Taeye SW, Tokatlian T, Torrents de la Pena A, Butera ST, LaBranche CC,
860 Montefiori DC, Silvestri G, Wilson IA, Irvine DJ, Sanders RW, Schief WR, Ward AB, Wyatt
861 RT, Barouch DH, Crotty S, Burton DR. 2017. Elicitation of robust Tier 2 neutralizing
862 antibody responses in non-human primates by HIV envelope trimer immunization using
863 optimized approaches. Immunity 46:1073-1088.E8.
864 https://doi.org/10.1016/j.immuni.2017.05.007.

865 7. Pauthner MG, Nkolola JP, Havenar-Daughton C, Murrell B, Reiss SM, Bastidas R, Prevost
866 J, Nedellec R, von Bredow B, Abbink P, Cottrell CA, Kulp DW, Tokatlian T, Nogal B,
867 Bianchi M, Li H, Lee JH, Butera ST, Evans DT, Hangartner L, Finzi A, Wilson IA, Wyatt RT,
868 Irvine DJ, Schief WR, Ward AB, Sanders RW, Crotty S, Shaw GM, Barouch DH, Burton DR.
869 2019. Vaccine-Induced protection from homologous tier 2 SHIV challenge in non-human
870 primates depends on serum-neutralizing antibody titers. Immunity 50:241-252.E6.
871 https://doi.org/10.1016/j.immuni.2018.11.011.

8. Felber BK, Lu Z, Hu X, Valentin A, Rosati M, Remmel CAL, Weiner JA, Carpenter MC, Faircloth K, Stanfield-Oakley S, Williams WB, Shen X, Tomaras GD, LaBranche CC, Montefiori D, Trinh HV, Rao M, Alam MS, Vandergrift NA, Saunders KO, Wang Y, Rountree W, Das J, Alter G, Reed SG, Aye PP, Schiro F, Pahar B, Dufour JP, Veazey RS, Marx PA, Venzon DJ, Shaw GM, Ferrari G, Ackerman ME, Haynes BF, Pavlakis GN. 2020. Co-immunization of DNA and protein in the same anatomical sites Induces superior protective immune responses against SHIV challenge. Cell Rep 31:107624. https://doi.org/10.1016/j.celrep.2020.107624.

9. Arunachalam PS, Charles TP, Joag V, Bollimpelli VS, Scott MKD, Wimmers F, Burton SL, Labranche CC, Petitdemange C, Gangadhara S, Styles TM, Quarnstrom CF, Walter KA, Ketas TJ, Legere T, Jagadeesh Reddy PB, Kasturi SP, Tsai A, Yeung BZ, Gupta S, Tomai M, Vasilakos J, Shaw GM, Kang CY, Moore JP, Subramaniam S, Khatri P, Montefiori D, Kozlowski PA, Derdeyn CA, Hunter E, Masopust D, Amara RR, Pulendran B. 2020. T cell-inducing vaccine durably prevents mucosal SHIV infection even with lower neutralizing antibody titers. Nat Med 26:932-940. https://doi.org/10.1038/s41591-020-0858-8.

10. Pegu A, Borate B, Huang Y, Pauthner MG, Hessell AJ, Julg B, Doria-Rose NA, Schmidt SD, Carpp LN, Cully MD, Chen X, Shaw GM, Barouch DH, Haigwood NL, Corey L, Burton DR, Roederer M, Gilbert PB, Mascola JR, Huang Y. 2019. A meta-analysis of passive immunization studies shows that serum-neutralizing antibody titer associates with protection against SHIV challenge. Cell Host Microbe 26:336-346.E3. https://doi.org/10.1016/j.chom.2019.08.014.

11. Corey L, Gilbert PB, Juraska M, Montefiori DC, Morris L, Karuna ST, Edupuganti S, Mgodi NM, deCamp AC, Rudnicki E, Huang Y, Gonzales P, Cabello R, Orrell C, Lama JR, Laher F, Lazarus EM, Sanchez J, Frank I, Hinojosa J, Sobieszczyk ME, Marshall KE, Mukwekwerere PG, Makhema J, Baden L, Mullins JI, Williamson C, Hural J, McElrath J, Bentley C, Takuva S, Lorenzo MMG, Burns DN, Espy N, Randhawa AK, Kochar N, Donnell DJ, Sista N, Andrew P, Kublin JG, Gray G, Ledgerwood JE, Mascola JR, Cohen MS. 2021. Antibody mediated prevention of HIV-1 acquisition in high-risk populations by the broadly neutralizing antibody VRC01. N Engl J Med XXX:YYY (in press).

12. Barouch DH, Whitney JB, Moldt B, Klein F, Oliveira TY, Liu J, Stephenson KE, Chang HW, Shekhar K, Gupta S, Nkolola JP, Seaman MS, Smith KM, Borducchi EN, Cabral C, Smith JY, Blackmore S, Sanisetty S, Perry JR, Beck M, Lewis MG, Rinaldi W, Chakraborty AK, Poignard P, Nussenzweig MC, Burton DR. 2013. Therapeutic efficacy of potent neutralizing HIV-1-specific monoclonal antibodies in SHIV-infected rhesus monkeys. Nature 503:224-8. https://doi.org/10.1038/nature12744.

13. Shingai M, Nishimura Y, Klein F, Mouquet H, Donau OK, Plishka R, Buckler-White A, Seaman M, Piatak M, Jr., Lifson JD, Dimitrov DS, Nussenzweig MC, Martin MA. 2013.

Antibody-mediated immunotherapy of macaques chronically infected with SHIV suppresses viraemia. Nature 503:277-80. https://doi.org/10.1038/nature12746.

14. Borducchi EN, Liu J, Nkolola JP, Cadena AM, Yu WH, Fischinger S, Broge T, Abbink P, Mercado NB, Chandrashekar A, Jetton D, Peter L, McMahan K, Moseley ET, Bekerman E, Hesselgesser J, Li W, Lewis MG, Alter G, Geleziunas R, Barouch DH. 2018. Antibody and TLR7 agonist delay viral rebound in SHIV-infected monkeys. Nature 563:360-364. https://doi.org/10.1038/s41586-018-0600-6.

15. Bender AM, Simonetti FR, Kumar MR, Fray EJ, Bruner KM, Timmons AE, Tai KY, Jenike KM, Antar AAR, Liu PT, Ho YC, Raugi DN, Seydi M, Gottlieb GS, Okoye AA, Del Prete GQ, Picker LJ, Mankowski JL, Lifson JD, Siliciano JD, Laird GM, Barouch DH, Clements JE, Siliciano RF. 2019. The landscape of persistent viral genomes in ART-treated SIV, SHIV, and HIV-2 infections. Cell Host Microbe 26:73-84.E4. https://doi.org/10.1016/j.chom.2019.06.005.

16. Dashti A, Waller C, Mavigner M, Schoof N, Bar KJ, Shaw GM, Vanderford TH, Liang S, Lifson JD, Dunham RM, Ferrari G, Tuyishime M, Lam CK, Nordstrom JL, Margolis DM, Silvestri G, Chahroudi A. 2020. SMAC mimetic plus triple-combination bispecific HIVxCD3 retargeting molecules in SHIV.C.CH505-infected, antiretroviral therapy-suppressed rhesus macaques. J Virol 94:e00793-20. https://doi.org/10.1128/JVI.00793-20.

17. Obregon-Perko V, Bricker K, Mensah G, Uddin F, Kumar M, Fray E, Siliciano RF, Schoof N, Horner A, Mavigner M, Liang S, Vanderford T, Sass J, Chan C, Berendam SJ, Bar K, Shaw GM, Silvestri G, Fouda G, Permar S, Chahroudi A. 2020. SHIV.C.CH505 persistence in ART-suppressed infant macaques is characterized by elevated SHIV RNA in the gut and high abundance of intact SHIV DNA in naive CD4+ T cells. J Virol 95:e01669-20. https://doi.org/10.1128/JVI.01669-20.

18. Harper J, Gordon S, Chan CN, Wang H, Lindemuth E, Galardi C, Falcinelli SD, Raines SLM, Read JL, Nguyen K, McGary CS, Nekorchuk M, Busman-Sahay K, Schawalder J, King C, Pino M, Micci L, Cervasi B, Jean S, Sanderson A, Johns B, Koblansky AA, Amrine-Madsen H, Lifson J, Margolis DM, Silvestri G, Bar KJ, Favre D, Estes JD, Paiardini M. 2020. CTLA-4 and PD-1 dual blockade induces SIV reactivation without control of rebound after antiretroviral therapy interruption. Nat Med 26:519-528. https://doi.org/10.1038/s41591-020-0782-y.

19. Saunders KO, Verkoczy LK, Jiang C, Zhang J, Parks R, Chen H, Housman M, Bouton-Verville H, Shen X, Trama AM, Scearce R, Sutherland L, Santra S, Newman A, Eaton A, Xu K, Georgiev IS, Joyce MG, Tomaras GD, Bonsignori M, Reed SG, Salazar A, Mascola JR, Moody MA, Cain DW, Centlivre M, Zurawski S, Zurawski G, Erickson HP, Kwong PD, Alam SM, Levy Y, Montefiori DC, Haynes BF. 2017. Vaccine induction of heterologous Tier 2

HIV-1 neutralizing antibodies in animal models. Cell Rep 21:3681-3690. https://doi.org/10.1016/j.celrep.2017.12.028.

20. Voss JE, Andrabi R, McCoy LE, de Val N, Fuller RP, Messmer T, Su CY, Sok D, Khan SN, Garces F, Pritchard LK, Wyatt RT, Ward AB, Crispin M, Wilson IA, Burton DR. 2017. Elicitation of neutralizing antibodies targeting the V2 apex of the HIV envelope trimer in a wild-type animal model. Cell Rep 21:222-235. https://doi.org/10.1016/j.celrep.2017.09.024.

21. Li J, Lord CI, Haseltine W, Letvin NL, Sodroski J. 1992. Infection of cynomolgus monkeys with a chimeric HIV-1/SIVmac virus that expresses the HIV-1 envelope glycoproteins. J Acquir Immune Defic Syndr (1988) 5:639-46.

22. Karlsson GB, Halloran M, Li J, Park IW, Gomila R, Reimann KA, Axthelm MK, Iliff SA, Letvin NL, Sodroski J. 1997. Characterization of molecularly cloned simian-human immunodeficiency viruses causing rapid CD4+ lymphocyte depletion in rhesus monkeys. J Virol 71:4218-25. https://doi.org/10.1128/JVI.71.6.4218-4225.1997.

23. Harouse JM, Gettie A, Eshetu T, Tan RC, Bohm R, Blanchard J, Baskin G, Cheng-Mayer C. 2001. Mucosal transmission and induction of simian AIDS by CCR5-specific simian/human immunodeficiency virus SHIV(SF162P3). J Virol 75:1990-5. https://doi.org/10.1128/JVI.75.4.1990-1995.2001.

24. Song RJ, Chenine AL, Rasmussen RA, Ruprecht CR, Mirshahidi S, Grisson RD, Xu W, Whitney JB, Goins LM, Ong H, Li PL, Shai-Kobiler E, Wang T, McCann CM, Zhang H, Wood C, Kankasa C, Secor WE, McClure HM, Strobert E, Else JG, Ruprecht RM. 2006. Molecularly cloned SHIV-1157ipd3N4: a highly replication-competent, mucosally transmissible R5 simian-human immunodeficiency virus encoding HIV clade C Env. J Virol 80:8729-38. https://doi.org/10.1128/JVI.00558-06.

25. Nishimura Y, Shingai M, Willey R, Sadjadpour R, Lee WR, Brown CR, Brenchley JM, Buckler-White A, Petros R, Eckhaus M, Hoffman V, Igarashi T, Martin MA. 2010. Generation of the pathogenic R5-tropic simian/human immunodeficiency virus SHIVAD8 by serial passaging in rhesus macaques. J Virol 84:4769-81. https://doi.org/10.1128/JVI.02279-09.

26. Warren CJ, Meyerson NR, Dirasantha O, Feldman ER, Wilkerson GK, Sawyer SL. 2019. Selective use of primate CD4 receptors by HIV-1. PLoS Biol 17:e3000304. https://doi.org/10.1371/journal.pbio.3000304.

27. Humes D, Emery S, Laws E, Overbaugh J. 2012. A species-specific amino acid difference in the macaque CD4 receptor restricts replication by global circulating HIV-1 variants

representing viruses from recent infection. J Virol 86:12472-83. https://doi.org/10.1128/JVI.02176-12.

28. Del Prete GQ, Keele BF, Fode J, Thummar K, Swanstrom AE, Rodriguez A, Raymond A, Estes JD, LaBranche CC, Montefiori DC, KewalRamani VN, Lifson JD, Bieniasz PD, Hatziioannou T. 2017. A single gp120 residue can affect HIV-1 tropism in macaques. PLoS Pathog 13:e1006572. https://doi.org/10.1371/journal.ppat.1006572.

29. O'Brien SP, Swanstrom AE, Pegu A, Ko SY, Immonen TT, Del Prete GQ, Fennessey CM, Gorman J, Foulds KE, Schmidt SD, Doria-Rose N, Williamson C, Hatziioannou T, Bieniasz PD, Li H, Shaw GM, Mascola JR, Koup RA, Kwong PD, Lifson JD, Roederer M, Keele BF. 2019. Rational design and in vivo selection of SHIVs encoding transmitted/founder subtype C HIV-1 envelopes. PLoS Pathog 15:e1007632. https://doi.org/10.1371/journal.ppat.1007632.

30. Finzi A, Pacheco B, Xiang SH, Pancera M, Herschhorn A, Wang L, Zeng X, Desormeaux A, Kwong PD, Sodroski J. 2012. Lineage-specific differences between human and simian immunodeficiency virus regulation of gp120 trimer association and CD4 binding. J Virol 86:8974-86. https://doi.org/10.1128/JVI.01076-12.

31. Xiang SH, Kwong PD, Gupta R, Rizzuto CD, Casper DJ, Wyatt R, Wang L, Hendrickson WA, Doyle ML, Sodroski J. 2002. Mutagenic stabilization and/or disruption of a CD4-bound state reveals distinct conformations of the human immunodeficiency virus type 1 gp120 envelope glycoprotein. J Virol 76:9888-99. https://doi.org/10.1128/jvi.76.19.9888-9899.2002.

32. Ding S, Medjahed H, Prevost J, Coutu M, Xiang SH, Finzi A. 2016. Lineage-specific differences between the gp120 inner domain layer 3 of human immunodeficiency virus and that of simian immunodeficiency virus. J Virol 90:10065-10073. https://doi.org/10.1128/JVI.01215-16.

33. Prevost J, Zoubchenok D, Richard J, Veillette M, Pacheco B, Coutu M, Brassard N, Parsons MS, Ruxrungtham K, Bunupuradah T, Tovanabutra S, Hwang KK, Moody MA, Haynes BF, Bonsignori M, Sodroski J, Kaufmann DE, Shaw GM, Chenine AL, Finzi A. 2017. Influence of the envelope gp120 phe 43 cavity on HIV-1 sensitivity to antibody-dependent cell-mediated cytotoxicity responses. J Virol 91:e02452-16. https://doi.org/10.1128/JVI.02452-16.

34. Prevost J, Tolbert WD, Medjahed H, Sherburn RT, Madani N, Zoubchenok D, Gendron-Lepage G, Gaffney AE, Grenier MC, Kirk S, Vergara N, Han C, Mann BT, Chenine AL, Ahmed A, Chaiken I, Kirchhoff F, Hahn BH, Haim H, Abrams CF, Smith AB, 3rd, Sodroski J,

1013 Pazgier M, Finzi A. 2020. The HIV-1 Env gp120 inner domains shapes the phe43 cavity
1014 and the CD4 binding site. mBio 11:e00280-20. https://doi.org/10.1128/mBio.00280-20.

1015 35. Li H, Wang S, Kong R, Ding W, Lee FH, Parker Z, Kim E, Learn GH, Hahn P, Policicchio B,
1016 Brocca-Cofano E, Deleage C, Hao X, Chuang GY, Gorman J, Gardner M, Lewis MG,
1017 Hatziioannou T, Santra S, Apetrei C, Pandrea I, Alam SM, Liao HX, Shen X, Tomaras GD,
1018 Farzan M, Chertova E, Keele BF, Estes JD, Lifson JD, Doms RW, Montefiori DC, Haynes BF,
1019 Sodroski JG, Kwong PD, Hahn BH, Shaw GM. 2016. Envelope residue 375 substitutions in
1020 simian-human immunodeficiency viruses enhance CD4 binding and replication in rhesus
1021 macaques. Proc Natl Acad Sci U S A 113:E3413-22.
1022 https://doi.org/10.1073/pnas.1606636113.

1023 36. Desormeaux A, Coutu M, Medjahed H, Pacheco B, Herschhorn A, Gu C, Xiang SH, Mao Y,
1024 Sodroski J, Finzi A. 2013. The highly conserved layer-3 component of the HIV-1 gp120
1025 inner domain is critical for CD4-required conformational transitions. J Virol 87:2549-62.
1026 https://doi.org/10.1128/JVI.03104-12.

1027 37. Finzi A, Xiang SH, Pacheco B, Wang L, Haight J, Kassa A, Danek B, Pancera M, Kwong PD,
1028 Sodroski J. 2010. Topological layers in the HIV-1 gp120 inner domain regulate gp41
1029 interaction and CD4-triggered conformational transitions. Mol Cell 37:656-67.
1030 https://doi.org/10.1016/j.molcel.2010.02.012.

1031 38. Roark RS, Li H, Williams WB, Chug H, Mason RD, Gorman J, Wang S, Lee FH, Rando J,
1032 Bonsignori M, Hwang KK, Saunders KO, Wiehe K, Moody MA, Hraber PT, Wagh K, Giorgi
1033 EE, Russell RM, Bibollet-Ruche F, Liu W, Connell J, Smith AG, DeVoto J, Murphy AI, Smith
1034 J, Ding W, Zhao C, Chohan N, Okumura M, Rosario C, Ding Y, Lindemuth E, Bauer AM,
1035 Bar KJ, Ambrozak D, Chao CW, Chuang GY, Geng H, Lin BC, Louder MK, Nguyen R, Zhang
1036 B, Lewis MG, Raymond D, Doria-Rose NA, Schramm CA, Douek DC, Roederer M, Kepler
1037 TB, Kelsoe G, et al. 2021. Recapitulation of HIV-1 Env-antibody coevolution in macaques
1038 leading to neutralization breadth. Science 371:eabd2638.
1039 https://doi.org/10.1126/science.abd2638.

1040 39. Poss M, Overbaugh J. 1999. Variants from the diverse virus population identified at
1041 seroconversion of a clade A human immunodeficiency virus type 1-infected woman
1042 have distinct biological properties. J Virol 73:5255-64.
1043 https://doi.org/10.1128/JVI.73.7.5255-5264.1999.

1044 40. Seaman MS, Janes H, Hawkins N, Grandpre LE, Devoy C, Giri A, Coffey RT, Harris L, Wood
1045 B, Daniels MG, Bhattacharya T, Lapedes A, Polonis VR, McCutchan FE, Gilbert PB, Self
1046 SG, Korber BT, Montefiori DC, Mascola JR. 2010. Tiered categorization of a diverse panel
1047 of HIV-1 Env pseudoviruses for assessment of neutralizing antibodies. J Virol 84:1439-52.
1048 https://doi.org/10.1128/JVI.02108-09.

41. deCamp A, Hraber P, Bailer RT, Seaman MS, Ochsenbauer C, Kappes J, Gottardo R, Edlefsen P, Self S, Tang H, Greene K, Gao H, Daniell X, Sarzotti-Kelsoe M, Gorny MK, Zolla-Pazner S, LaBranche CC, Mascola JR, Korber BT, Montefiori DC. 2014. Global panel of HIV-1 Env reference strains for standardized assessments of vaccine-elicited neutralizing antibodies. J Virol 88:2489-507. https://doi.org/10.1128/JVI.02853-13.

42. Hraber P, Seaman MS, Bailer RT, Mascola JR, Montefiori DC, Korber BT. 2014. Prevalence of broadly neutralizing antibody responses during chronic HIV-1 infection. AIDS 28:163-9. https://doi.org/10.1097/QAD.0000000000000106.

43. Abrahams MR, Anderson JA, Giorgi EE, Seoighe C, Mlisana K, Ping LH, Athreya GS, Treurnicht FK, Keele BF, Wood N, Salazar-Gonzalez JF, Bhattacharya T, Chu H, Hoffman I, Galvin S, Mapanje C, Kazembe P, Thebus R, Fiscus S, Hide W, Cohen MS, Karim SA, Haynes BF, Shaw GM, Hahn BH, Korber BT, Swanstrom R, Williamson C, Team CAIS, Center for HIVAVIC. 2009. Quantitating the multiplicity of infection with human immunodeficiency virus type 1 subtype C reveals a non-poisson distribution of transmitted variants. J Virol 83:3556-67. https://doi.org/10.1128/JVI.02132-08.

44. Liao HX, Tsao CY, Alam SM, Muldoon M, Vandergrift N, Ma BJ, Lu X, Sutherland LL, Scearce RM, Bowman C, Parks R, Chen H, Blinn JH, Lapedes A, Watson S, Xia SM, Foulger A, Hahn BH, Shaw GM, Swanstrom R, Montefiori DC, Gao F, Haynes BF, Korber B. 2013. Antigenicity and immunogenicity of transmitted/founder, consensus, and chronic envelope glycoproteins of human immunodeficiency virus type 1. J Virol 87:4185-201. https://doi.org/10.1128/JVI.02297-12.

45. Alexander J, Mendy J, Vang L, Avanzini JB, Garduno F, Manayani DJ, Ishioka G, Farness P, Ping LH, Swanstrom R, Parks R, Liao HX, Haynes BF, Montefiori DC, LaBranche C, Smith J, Gurwith M, Mayall T. 2013. Pre-clinical development of a recombinant, replication-competent adenovirus serotype 4 vector vaccine expressing HIV-1 envelope 1086 clade C. PLoS One 8:e82380. https://doi.org/10.1371/journal.pone.0082380.

46. Zambonelli C, Dey AK, Hilt S, Stephenson S, Go EP, Clark DF, Wininger M, Labranche C, Montefiori D, Liao HX, Swanstrom RI, Desaire H, Haynes BF, Carfi A, Barnett SW. 2016. Generation and characterization of a bivalent HIV-1 Subtype C gp120 protein boost for proof-of-concept HIV vaccine efficacy trials in southern Africa. PLoS One 11:e0157391. https://doi.org/10.1371/journal.pone.0157391.

47. Pugach P, Ozorowski G, Cupo A, Ringe R, Yasmeen A, de Val N, Derking R, Kim HJ, Korzun J, Golabek M, de Los Reyes K, Ketas TJ, Julien JP, Burton DR, Wilson IA, Sanders RW, Klasse PJ, Ward AB, Moore JP. 2015. A native-like SOSIP.664 trimer based on an HIV-1 subtype B env gene. J Virol 89:3380-95. https://doi.org/10.1128/JVI.03473-14.

48. Kijak GH, Sanders-Buell E, Chenine AL, Eller MA, Goonetilleke N, Thomas R, Leviyang S, Harbolick EA, Bose M, Pham P, Oropeza C, Poltavee K, O'Sullivan AM, Billings E, Merbah M, Costanzo MC, Warren JA, Slike B, Li H, Peachman KK, Fischer W, Gao F, Cicala C, Arthos J, Eller LA, O'Connell RJ, Sinei S, Maganga L, Kibuuka H, Nitayaphan S, Rao M, Marovich MA, Krebs SJ, Rolland M, Korber BT, Shaw GM, Michael NL, Robb ML, Tovanabutra S, Kim JH. 2017. Rare HIV-1 transmitted/founder lineages identified by deep viral sequencing contribute to rapid shifts in dominant quasispecies during acute and early infection. PLoS Pathog 13:e1006510. https://doi.org/10.1371/journal.ppat.1006510.

49. Rolland M, Tovanabutra S, Dearlove B, Li Y, Owen CL, Lewitus E, Sanders-Buell E, Bose M, O'Sullivan A, Rossenkhan R, Labuschagne JPL, Edlefsen PT, Reeves DB, Kijak G, Miller S, Poltavee K, Lee J, Bonar L, Harbolick E, Ahani B, Pham P, Kibuuka H, Maganga L, Nitayaphan S, Sawe FK, Eller LA, Gramzinski R, Kim JH, Michael NL, Robb ML, Team RVS. 2020. Molecular dating and viral load growth rates suggested that the eclipse phase lasted about a week in HIV-1 infected adults in East Africa and Thailand. PLoS Pathog 16:e1008179. https://doi.org/10.1371/journal.ppat.1008179.

50. Wagh K, Kreider EF, Li Y, Barbian HJ, Learn GH, Giorgi E, Hraber PT, Decker TG, Smith AG, Gondim MV, Gillis L, Wandzilak J, Chuang GY, Rawi R, Cai F, Pellegrino P, Williams I, Overbaugh J, Gao F, Kwong PD, Haynes BF, Shaw GM, Borrow P, Seaman MS, Hahn BH, Korber B. 2018. Completeness of HIV-1 envelope glycan shield at transmission determines neutralization breadth. Cell Rep 25:893-908.E7. https://doi.org/10.1016/j.celrep.2018.09.087.

51. Rademeyer C, Korber B, Seaman MS, Giorgi EE, Thebus R, Robles A, Sheward DJ, Wagh K, Garrity J, Carey BR, Gao H, Greene KM, Tang H, Bandawe GP, Marais JC, Diphoko TE, Hraber P, Tumba N, Moore PL, Gray GE, Kublin J, McElrath MJ, Vermeulen M, Middelkoop K, Bekker LG, Hoelscher M, Maboko L, Makhema J, Robb ML, Abdool Karim S, Abdool Karim Q, Kim JH, Hahn BH, Gao F, Swanstrom R, Morris L, Montefiori DC, Williamson C. 2016. Features of recently transmitted HIV-1 clade C viruses that impact antibody recognition: implications for active and passive immunization. PLoS Pathog 12:e1005742. https://doi.org/10.1371/journal.ppat.1005742.

52. Bonsignori M, Hwang KK, Chen X, Tsao CY, Morris L, Gray E, Marshall DJ, Crump JA, Kapiga SH, Sam NE, Sinangil F, Pancera M, Yongping Y, Zhang B, Zhu J, Kwong PD, O'Dell S, Mascola JR, Wu L, Nabel GJ, Phogat S, Seaman MS, Whitesides JF, Moody MA, Kelsoe G, Yang X, Sodroski J, Shaw GM, Montefiori DC, Kepler TB, Tomaras GD, Alam SM, Liao HX, Haynes BF. 2011. Analysis of a clonal lineage of HIV-1 envelope V2/V3 conformational epitope-specific broadly neutralizing antibodies and their inferred unmutated common ancestors. J Virol 85:9998-10009. https://doi.org/10.1128/JVI.05045-11.

53. Andrabi R, Voss JE, Liang CH, Briney B, McCoy LE, Wu CY, Wong CH, Poignard P, Burton DR. 2015. Identification of Common Features in Prototype Broadly Neutralizing Antibodies to HIV Envelope V2 Apex to Facilitate Vaccine Design. Immunity 43:959-73. https://doi.org/10.1016/j.immuni.2015.10.014.

54. Gorman J, Soto C, Yang MM, Davenport TM, Guttman M, Bailer RT, Chambers M, Chuang GY, DeKosky BJ, Doria-Rose NA, Druz A, Ernandes MJ, Georgiev IS, Jarosinski MC, Joyce MG, Lemmin TM, Leung S, Louder MK, McDaniel JR, Narpala S, Pancera M, Stuckey J, Wu X, Yang Y, Zhang B, Zhou T, Program NCS, Mullikin JC, Baxa U, Georgiou G, McDermott AB, Bonsignori M, Haynes BF, Moore PL, Morris L, Lee KK, Shapiro L, Mascola JR, Kwong PD. 2016. Structures of HIV-1 Env V1V2 with broadly neutralizing antibodies reveal commonalities that enable vaccine design. Nat Struct Mol Biol 23:81-90. https://doi.org/10.1038/nsmb.3144.

55. Wu X, Parast AB, Richardson BA, Nduati R, John-Stewart G, Mbori-Ngacha D, Rainwater SM, Overbaugh J. 2006. Neutralization escape variants of human immunodeficiency virus type 1 are transmitted from mother to infant. J Virol 80:835-44. https://doi.org/10.1128/JVI.80.2.835-844.2006.

56. Goo L, Chohan V, Nduati R, Overbaugh J. 2014. Early development of broadly neutralizing antibodies in HIV-1-infected infants. Nat Med 20:655-8. https://doi.org/10.1038/nm.3565.

57. Li Y, Kappes JC, Conway JA, Price RW, Shaw GM, Hahn BH. 1991. Molecular characterization of human immunodeficiency virus type 1 cloned directly from uncultured human brain tissue: identification of replication-competent and -defective viral genomes. J Virol 65:3973-85. https://doi.org/10.1128/JVI.65.8.3973-3985.1991.

58. Li Y, Hui H, Burgess CJ, Price RW, Sharp PM, Hahn BH, Shaw GM. 1992. Complete nucleotide sequence, genome organization, and biological properties of human immunodeficiency virus type 1 in vivo: evidence for limited defectiveness and complementation. J Virol 66:6587-600. https://doi.org/10.1128/JVI.66.11.6587-6600.1992.

59. Liao HX, Lynch R, Zhou T, Gao F, Alam SM, Boyd SD, Fire AZ, Roskin KM, Schramm CA, Zhang Z, Zhu J, Shapiro L, Program NCS, Mullikin JC, Gnanakaran S, Hraber P, Wiehe K, Kelsoe G, Yang G, Xia SM, Montefiori DC, Parks R, Lloyd KE, Scearce RM, Soderberg KA, Cohen M, Kamanga G, Louder MK, Tran LM, Chen Y, Cai F, Chen S, Moquin S, Du X, Joyce MG, Srivatsan S, Zhang B, Zheng A, Shaw GM, Hahn BH, Kepler TB, Korber BT, Kwong PD, Mascola JR, Haynes BF. 2013. Co-evolution of a broadly neutralizing HIV-1 antibody and founder virus. Nature 496:469-76. https://doi.org/10.1038/nature12053.

60. Bonsignori M, Kreider EF, Fera D, Meyerhoff RR, Bradley T, Wiehe K, Alam SM, Aussedat B, Walkowicz WE, Hwang KK, Saunders KO, Zhang R, Gladden MA, Monroe A, Kumar A, Xia SM, Cooper M, Louder MK, McKee K, Bailer RT, Pier BW, Jette CA, Kelsoe G, Williams WB, Morris L, Kappes J, Wagh K, Kamanga G, Cohen MS, Hraber PT, Montefiori DC, Trama A, Liao HX, Kepler TB, Moody MA, Gao F, Danishefsky SJ, Mascola JR, Shaw GM, Hahn BH, Harrison SC, Korber BT, Haynes BF. 2017. Staged induction of HIV-1 glycan-dependent broadly neutralizing antibodies. Sci Transl Med 9:eaai7514. https://doi.org/10.1126/scitranslmed.aai7514.

61. Sanders RW, Derking R, Cupo A, Julien JP, Yasmeen A, de Val N, Kim HJ, Blattner C, de la Pena AT, Korzun J, Golabek M, de Los Reyes K, Ketas TJ, van Gils MJ, King CR, Wilson IA, Ward AB, Klasse PJ, Moore JP. 2013. A next-generation cleaved, soluble HIV-1 Env trimer, BG505 SOSIP.664 gp140, expresses multiple epitopes for broadly neutralizing but not non-neutralizing antibodies. PLoS Pathog 9:e1003618. https://doi.org/10.1371/journal.ppat.1003618.

62. Moore PL, Sheward D, Nonyane M, Ranchobe N, Hermanus T, Gray ES, Abdool Karim SS, Williamson C, Morris L. 2013. Multiple pathways of escape from HIV broadly cross-neutralizing V2-dependent antibodies. J Virol 87:4882-94. https://doi.org/10.1128/JVI.03424-12.

63. Baalwa J, Wang S, Parrish NF, Decker JM, Keele BF, Learn GH, Yue L, Ruzagira E, Ssemwanga D, Kamali A, Amornkul PN, Price MA, Kappes JC, Karita E, Kaleebu P, Sanders E, Gilmour J, Allen S, Hunter E, Montefiori DC, Haynes BF, Cormier E, Hahn BH, Shaw GM. 2013. Molecular identification, cloning and characterization of transmitted/founder HIV-1 subtype A, D and A/D infectious molecular clones. Virology 436:33-48. https://doi.org/10.1016/j.virol.2012.10.009.

64. Li M, Salazar-Gonzalez JF, Derdeyn CA, Morris L, Williamson C, Robinson JE, Decker JM, Li Y, Salazar MG, Polonis VR, Mlisana K, Karim SA, Hong K, Greene KM, Bilska M, Zhou J, Allen S, Chomba E, Mulenga J, Vwalika C, Gao F, Zhang M, Korber BT, Hunter E, Hahn BH, Montefiori DC. 2006. Genetic and neutralization properties of subtype C human immunodeficiency virus type 1 molecular env clones from acute and early heterosexually acquired infections in Southern Africa. J Virol 80:11776-90. https://doi.org/10.1128/JVI.01730-06.

65. Del Prete GQ, Ailers B, Moldt B, Keele BF, Estes JD, Rodriguez A, Sampias M, Oswald K, Fast R, Trubey CM, Chertova E, Smedley J, LaBranche CC, Montefiori DC, Burton DR, Shaw GM, Markowitz M, Piatak M, Jr., KewalRamani VN, Bieniasz PD, Lifson JD, Hatziioannou T. 2014. Selection of unadapted, pathogenic SHIVs encoding newly transmitted HIV-1 envelope proteins. Cell Host Microbe 16:412-8. https://doi.org/10.1016/j.chom.2014.08.003.

66. Boyd DF, Peterson D, Haggarty BS, Jordan AP, Hogan MJ, Goo L, Hoxie JA, Overbaugh J. 2015. Mutations in HIV-1 envelope that enhance entry with the macaque CD4 receptor alter antibody recognition by disrupting quaternary interactions within the trimer. J Virol 89:894-907. https://doi.org/10.1128/JVI.02680-14.

67. Phillips AN. 1996. Reduction of HIV concentration during acute infection: independence from a specific immune response. Science 271:497-9. https://doi.org/10.1126/science.271.5248.497.

68. Nowak MA, Lloyd AL, Vasquez GM, Wiltrout TA, Wahl LM, Bischofberger N, Williams J, Kinter A, Fauci AS, Hirsch VM, Lifson JD. 1997. Viral dynamics of primary viremia and antiretroviral therapy in simian immunodeficiency virus infection. J Virol 71:7518-25. https://doi.org/10.1128/JVI.71.10.7518-7525.1997.

69. Ndhlovu ZM, Kamya P, Mewalal N, Kloverpris HN, Nkosi T, Pretorius K, Laher F, Ogunshola F, Chopera D, Shekhar K, Ghebremichael M, Ismail N, Moodley A, Malik A, Leslie A, Goulder PJ, Buus S, Chakraborty A, Dong K, Ndung'u T, Walker BD. 2015. Magnitude and Kinetics of CD8+ T Cell Activation during Hyperacute HIV Infection Impact Viral Set Point. Immunity 43:591-604. https://doi.org/10.1016/j.immuni.2015.08.012.

70. Robb ML, Eller LA, Kibuuka H, Rono K, Maganga L, Nitayaphan S, Kroon E, Sawe FK, Sinei S, Sriplienchan S, Jagodzinski LL, Malia J, Manak M, de Souza MS, Tovanabutra S, Sanders-Buell E, Rolland M, Dorsey-Spitz J, Eller MA, Milazzo M, Li Q, Lewandowski A, Wu H, Swann E, O'Connell RJ, Peel S, Dawson P, Kim JH, Michael NL, Team RVS. 2016. Prospective study of Acute HIV-1 infection in adults in East Africa and Thailand. N Engl J Med 374:2120-30. https://doi.org/10.1056/NEJMoa1508952.

71. Markowitz M, Louie M, Hurley A, Sun E, Di Mascio M, Perelson AS, Ho DD. 2003. A novel antiviral intervention results in more accurate assessment of human immunodeficiency virus type 1 replication dynamics and T-cell decay in vivo. J Virol 77:5037-8. https://doi.org/10.1128/jvi.77.8.5037-5038.2003.

72. Decker JM, Bibollet-Ruche F, Wei X, Wang S, Levy DN, Wang W, Delaporte E, Peeters M, Derdeyn CA, Allen S, Hunter E, Saag MS, Hoxie JA, Hahn BH, Kwong PD, Robinson JE, Shaw GM. 2005. Antigenic conservation and immunogenicity of the HIV coreceptor binding site. J Exp Med 201:1407-19. https://doi.org/10.1084/jem.20042510.

73. Keele BF, Giorgi EE, Salazar-Gonzalez JF, Decker JM, Pham KT, Salazar MG, Sun C, Grayson T, Wang S, Li H, Wei X, Jiang C, Kirchherr JL, Gao F, Anderson JA, Ping LH, Swanstrom R, Tomaras GD, Blattner WA, Goepfert PA, Kilby JM, Saag MS, Delwart EL, Busch MP, Cohen MS, Montefiori DC, Haynes BF, Gaschen B, Athreya GS, Lee HY, Wood

N, Seoighe C, Perelson AS, Bhattacharya T, Korber BT, Hahn BH, Shaw GM. 2008. Identification and characterization of transmitted and early founder virus envelopes in primary HIV-1 infection. Proc Natl Acad Sci U S A 105:7552-7. https://doi.org/10.1073/pnas.0802203105.

74. Davis KL, Bibollet-Ruche F, Li H, Decker JM, Kutsch O, Morris L, Salomon A, Pinter A, Hoxie JA, Hahn BH, Kwong PD, Shaw GM. 2009. Human immunodeficiency virus type 2 (HIV-2)/HIV-1 envelope chimeras detect high titers of broadly reactive HIV-1 V3-specific antibodies in human plasma. J Virol 83:1240-59. https://doi.org/10.1128/JVI.01743-08.

75. Del Prete GQ, Scarlotta M, Newman L, Reid C, Parodi LM, Roser JD, Oswald K, Marx PA, Miller CJ, Desrosiers RC, Barouch DH, Pal R, Piatak M, Jr., Chertova E, Giavedoni LD, O'Connor DH, Lifson JD, Keele BF. 2013. Comparative characterization of transfection- and infection-derived simian immunodeficiency virus challenge stocks for in vivo nonhuman primate studies. J Virol 87:4584-95. https://doi.org/10.1128/JVI.03507-12.

76. Louder MK, Sambor A, Chertova E, Hunte T, Barrett S, Ojong F, Sanders-Buell E, Zolla-Pazner S, McCutchan FE, Roser JD, Gabuzda D, Lifson JD, Mascola JR. 2005. HIV-1 envelope pseudotyped viral vectors and infectious molecular clones expressing the same envelope glycoprotein have a similar neutralization phenotype, but culture in peripheral blood mononuclear cells is associated with decreased neutralization sensitivity. Virology 339:226-38. https://doi.org/10.1016/j.virol.2005.06.003.

77. Cohen YZ, Lorenzi JCC, Seaman MS, Nogueira L, Schoofs T, Krassnig L, Butler A, Millard K, Fitzsimons T, Daniell X, Dizon JP, Shimeliovich I, Montefiori DC, Caskey M, Nussenzweig MC. 2018. Neutralizing activity of broadly neutralizing anti-HIV-1 antibodies against clade B clinical isolates produced in peripheral blood mononuclear cells. J Virol 92:e01883-17. https://doi.org/10.1128/JVI.01883-17.

78. Patel P, Borkowf CB, Brooks JT, Lasry A, Lansky A, Mermin J. 2014. Estimating per-act HIV transmission risk: a systematic review. AIDS 28:1509-19. https://doi.org/10.1097/QAD.0000000000000298.

79. Sok D, Burton DR. 2018. Recent progress in broadly neutralizing antibodies to HIV. Nat Immunol 19:1179-1188. https://doi.org/10.1038/s41590-018-0235-7.

80. Steichen JM, Lin YC, Havenar-Daughton C, Pecetta S, Ozorowski G, Willis JR, Toy L, Sok D, Liguori A, Kratochvil S, Torres JL, Kalyuzhniy O, Melzi E, Kulp DW, Raemisch S, Hu X, Bernard SM, Georgeson E, Phelps N, Adachi Y, Kubitz M, Landais E, Umotoy J, Robinson A, Briney B, Wilson IA, Burton DR, Ward AB, Crotty S, Batista FD, Schief WR. 2019. A generalized HIV vaccine design strategy for priming of broadly neutralizing antibody responses. Science 366:eaax4380. https://doi.org/10.1126/science.aax4380.

1264 81. Kwong PD, Mascola JR. 2018. HIV-1 Vaccines Based on Antibody Identification, B Cell
1265 Ontogeny, and Epitope Structure. Immunity 48:855-871.
1266 https://doi.org/10.1016/j.immuni.2018.04.029.

1267 82. Haynes BF, Burton DR, Mascola JR. 2019. Multiple roles for HIV broadly neutralizing
1268 antibodies. Sci Transl Med 11:eaaz2686. https://doi.org/10.1126/scitranslmed.aaz2686.

1269 83. Ou L, Kong WP, Chuang GY, Ghosh M, Gulla K, O'Dell S, Varriale J, Barefoot N, Changela
1270 A, Chao CW, Cheng C, Druz A, Kong R, McKee K, Rawi R, Sarfo EK, Schon A, Shaddeau A,
1271 Tsybovsky Y, Verardi R, Wang S, Wanninger TG, Xu K, Yang GJ, Zhang B, Zhang Y, Zhou T,
1272 Program VRCP, Arnold FJ, Doria-Rose NA, Lei QP, Ryan ET, Vann WF, Mascola JR, Kwong
1273 PD. 2020. Preclinical development of a fusion peptide conjugate as an HIV vaccine
1274 immunogen. Sci Rep 10:3032. https://doi.org/10.1038/s41598-020-59711-y.

1275 84. Consortium RMGSaA, Gibbs RA, Rogers J, Katze MG, Bumgarner R, Weinstock GM,
1276 Mardis ER, Remington KA, Strausberg RL, Venter JC, Wilson RK, Batzer MA, Bustamante
1277 CD, Eichler EE, Hahn MW, Hardison RC, Makova KD, Miller W, Milosavljevic A, Palermo
1278 RE, Siepel A, Sikela JM, Attaway T, Bell S, Bernard KE, Buhay CJ, Chandrabose MN, Dao
1279 M, Davis C, Delehaunty KD, Ding Y, Dinh HH, Dugan-Rocha S, Fulton LA, Gabisi RA,
1280 Garner TT, Godfrey J, Hawes AC, Hernandez J, Hines S, Holder M, Hume J, Jhangiani SN,
1281 Joshi V, Khan ZM, Kirkness EF, Cree A, Fowler RG, Lee S, Lewis LR, et al. 2007.
1282 Evolutionary and biomedical insights from the rhesus macaque genome. Science
1283 316:222-34. https://doi.org/10.1126/science.1139247.

1284 85. Ramesh A, Darko S, Hua A, Overman G, Ransier A, Francica JR, Trama A, Tomaras GD,
1285 Haynes BF, Douek DC, Kepler TB. 2017. Structure and diversity of the rhesus macaque
1286 Immunoglobulin loci through multiple de novo genome assemblies. Front Immunol
1287 8:1407. https://doi.org/10.3389/fimmu.2017.01407.

1288 86. Goonetilleke N, Liu MK, Salazar-Gonzalez JF, Ferrari G, Giorgi E, Ganusov VV, Keele BF,
1289 Learn GH, Turnbull EL, Salazar MG, Weinhold KJ, Moore S, B CCC, Letvin N, Haynes BF,
1290 Cohen MS, Hraber P, Bhattacharya T, Borrow P, Perelson AS, Hahn BH, Shaw GM, Korber
1291 BT, McMichael AJ. 2009. The first T cell response to transmitted/founder virus
1292 contributes to the control of acute viremia in HIV-1 infection. J Exp Med 206:1253-72.
1293 https://doi.org/10.1084/jem.20090365.

1294 87. Salazar-Gonzalez JF, Salazar MG, Keele BF, Learn GH, Giorgi EE, Li H, Decker JM, Wang S,
1295 Baalwa J, Kraus MH, Parrish NF, Shaw KS, Guffey MB, Bar KJ, Davis KL, Ochsenbauer-
1296 Jambor C, Kappes JC, Saag MS, Cohen MS, Mulenga J, Derdeyn CA, Allen S, Hunter E,
1297 Markowitz M, Hraber P, Perelson AS, Bhattacharya T, Haynes BF, Korber BT, Hahn BH,
1298 Shaw GM. 2009. Genetic identity, biological phenotype, and evolutionary pathways of

transmitted/founder viruses in acute and early HIV-1 infection. J Exp Med 206:1273-89. https://doi.org/10.1084/jem.20090378.

88. Wyatt R, Kwong PD, Desjardins E, Sweet RW, Robinson J, Hendrickson WA, Sodroski JG. 1998. The antigenic structure of the HIV gp120 envelope glycoprotein. Nature 393:705-11. https://doi.org/10.1038/31514.

89. Starcich BR, Hahn BH, Shaw GM, McNeely PD, Modrow S, Wolf H, Parks ES, Parks WP, Josephs SF, Gallo RC, et al. 1986. Identification and characterization of conserved and variable regions in the envelope gene of HTLV-III/LAV, the retrovirus of AIDS. Cell 45:637-48. https://doi.org/10.1016/0092-8674(86)90778-6.

90. Kwong PD, Doyle ML, Casper DJ, Cicala C, Leavitt SA, Majeed S, Steenbeke TD, Venturi M, Chaiken I, Fung M, Katinger H, Parren PW, Robinson J, Van Ryk D, Wang L, Burton DR, Freire E, Wyatt R, Sodroski J, Hendrickson WA, Arthos J. 2002. HIV-1 evades antibody-mediated neutralization through conformational masking of receptor-binding sites. Nature 420:678-82. https://doi.org/10.1038/nature01188.

91. Wei X, Decker JM, Wang S, Hui H, Kappes JC, Wu X, Salazar-Gonzalez JF, Salazar MG, Kilby JM, Saag MS, Komarova NL, Nowak MA, Hahn BH, Kwong PD, Shaw GM. 2003. Antibody neutralization and escape by HIV-1. Nature 422:307-12. https://doi.org/10.1038/nature01470.

92. Holmes EC. 2003. Error thresholds and the constraints to RNA virus evolution. Trends Microbiol 11:543-6. https://doi.org/10.1016/j.tim.2003.10.006.

93. Woo J, Robertson DL, Lovell SC. 2010. Constraints on HIV-1 diversity from protein structure. J Virol 84:12995-3003. https://doi.org/10.1128/JVI.00702-10.

94. Haddox HK, Dingens AS, Bloom JD. 2016. Experimental estimation of the effects of all amino-acid Mutations to HIV's envelope protein on viral replication in cell culture. PLoS Pathog 12:e1006114. https://doi.org/10.1371/journal.ppat.1006114.

95. Moore PL. 2018. The neutralizing antibody response to the HIV-1 Env protein. Curr HIV Res 16:21-28. https://doi.org/10.2174/1570162X15666171124122044.

96. Han Q, Jones JA, Nicely NI, Reed RK, Shen X, Mansouri K, Louder M, Trama AM, Alam SM, Edwards RJ, Bonsignori M, Tomaras GD, Korber B, Montefiori DC, Mascola JR, Seaman MS, Haynes BF, Saunders KO. 2019. Difficult-to-neutralize global HIV-1 isolates are neutralized by antibodies targeting open envelope conformations. Nat Commun 10:2898. https://doi.org/10.1038/s41467-019-10899-2.

97. Tartaglia LJ, Gupte S, Pastores KC, Trott S, Abbink P, Mercado NB, Li Z, Liu PT, Borducchi EN, Chandrashekar A, Bondzie EA, Hamza V, Kordana N, Mahrokhian S, Lavine CL, Seaman MS, Li H, Shaw GM, Barouch DH. 2020. Differential outcomes following optimization of simian-human immunodeficiency viruses from clades AE, B, and C. J Virol 94:e01860-19. https://doi.org/10.1128/JVI.01860-19.

98. Keele BF, Li H, Learn GH, Hraber P, Giorgi EE, Grayson T, Sun C, Chen Y, Yeh WW, Letvin NL, Mascola JR, Nabel GJ, Haynes BF, Bhattacharya T, Perelson AS, Korber BT, Hahn BH, Shaw GM. 2009. Low-dose rectal inoculation of rhesus macaques by SIVsmE660 or SIVmac251 recapitulates human mucosal infection by HIV-1. J Exp Med 206:1117-34. https://doi.org/10.1084/jem.20082831.

99. Deleage C, Immonen TT, Fennessey CM, Reynaldi A, Reid C, Newman L, Lipkey L, Schlub TE, Camus C, O'Brien S, Smedley J, Conway JM, Del Prete GQ, Davenport MP, Lifson JD, Estes JD, Keele BF. 2019. Defining early SIV replication and dissemination dynamics following vaginal transmission. Sci Adv 5:eaav7116. https://doi.org/10.1126/sciadv.aav7116.

100. Bar KJ, Coronado E, Hensley-McBain T, O'Connor MA, Osborn JM, Miller C, Gott TM, Wangari S, Iwayama N, Ahrens CY, Smedley J, Moats C, Lynch RM, Haddad EK, Haigwood NL, Fuller DH, Shaw GM, Klatt NR, Manuzak JA. 2019. Simian-human immunodeficiency virus SHIV.CH505 infection of rhesus macaques results in persistent viral replication and induces intestinal immunopathology. J Virol 93:e00372-19. https://doi.org/10.1128/JVI.00372-19.

101. Bauer AM, Ziani W, Lindemuth E, Kuri-Cervantes L, Li H, Lee FH, Watkins M, Ding W, Xu H, Veazey R, Bar KJ. 2020. Novel Transmitted/Founder Simian-Human Immunodeficiency Viruses for Human Immunodeficiency Virus Latency and Cure Research. J Virol 94:e01659. https://doi.org/10.1128/JVI.01659-19.

102. Sarzotti-Kelsoe M, Bailer RT, Turk E, Lin CL, Bilska M, Greene KM, Gao H, Todd CA, Ozaki DA, Seaman MS, Mascola JR, Montefiori DC. 2014. Optimization and validation of the TZM-bl assay for standardized assessments of neutralizing antibodies against HIV-1. J Immunol Methods 409:131-46. https://doi.org/10.1016/j.jim.2013.11.022.

103. Song H, Giorgi EE, Ganusov VV, Cai F, Athreya G, Yoon H, Carja O, Hora B, Hraber P, Romero-Severson E, Jiang C, Li X, Wang S, Li H, Salazar-Gonzalez JF, Salazar MG, Goonetilleke N, Keele BF, Montefiori DC, Cohen MS, Shaw GM, Hahn BH, McMichael AJ, Haynes BF, Korber B, Bhattacharya T, Gao F. 2018. Tracking HIV-1 recombination to resolve its contribution to HIV-1 evolution in natural infection. Nat Commun 9:1928. https://doi.org/10.1038/s41467-018-04217-5.

1367
1368
1369

Figure Legends

Figure 1. First (**A**) and second (**B**) generation design schemes for SHIV constructions. The first generation design (35) consists of a proviral backbone of SIVmac766 (a T/F clone derived from the SIVmac251 isolate) shown in grey and HIV-1.D.191859 shown in red. A *vpu-env* amplicon is subcloned into this plasmid vector as describe (35). Note in the expanded figures in panel A that the proviral backbone design results in duplications of SIV and HIV-1 *tat1* and gp41 sequences (indicated by slash marks) that are spontaneously deleted during *in vivo* replication of the SHIVs (**Fig. 2**). The second generation design scheme (panel B) eliminates these duplications and adds a *BSMBI* cloning site that allows for simple introduction of either a *vpu-env* amplicon or *env* amplicon.

Figure 2. Spontaneous deletion of redundant *tat1 and env* gp41 sequences from the version 1 SHIV proviral backbone in SHIV.C.CH505 infected monkey RM6072. (**A**) Expanded segments of the *vpr – tat1* gene overlap and *tat2 – rev2 – env – nef gene* overlap from **Fig. 1A** are illustrated above Pixel plots (https://www.hiv.lanl.gov/content/sequence/pixel/pixel.html) of 39 single genome sequences from RM6072 20 weeks post-SHIV infection and 26 sequences 32 weeks post-SHIV infection. A 68 bp deletion of redundant sequences in *tat1* and a 21 bp deletion of redundant sequences in *env* gp41 rapidly becomes fixed in the evolving virus quasispecies. The version 2 backbone vector eliminates these redundant sequences. (**B**) Nucleotide and inferred amino acid sequences of the junctional regions of HIV-1 and SIV *tat1 and env* gp41 version 1 and 2 backbone vectors are shown, highlighting the differences in their designs.

Figure 3. Replication kinetics of SHIVs bearing ten different HIV-1 Envs with allelic variants at residue Env375 (S-Ser, M-Met, Y-Tyr, H-His, W-Trp, F-Phe, T-Thr) in cell culture. Primary,

activated human and rhesus $CD4^+$ T cells were inoculated with 293T-derived SHIVs and culture supernatants were sampled on the days indicated. Panels display results of representative experiments, which were reproduced in large scale expansions of SHIVs in rhesus $CD4^+$ T cells *in vitro* (**Table 2**) and in RMs *in vivo* (**Fig. 4**).

Figure 4. Plasma vRNA kinetics following intravenous inoculation of RMs with SHIVs bearing six Env 375 allelic variants. Open symbols denote animals that were treated with anti-CD8 mAb at week 0. Solid black symbols denote animals that were not treated with anti-CD8 mAb at week 0. Some animals were treated with anti-CD8 mAb at time points indicated during the course of SHIV infection and these animals are indicated by a shift in solid symbols from black to blue. Pie diagrams represent >5,000 vRNA/cDNA sequences and indicate the proportions of different Env375 alleles in plasma vRNA 2 and 4 weeks after SHIV inoculations. Where pie diagrams are not shown, animals were inoculated with SHIVs containing a single Env375 allele (**Table 3**).

Figure 5. Comparison of replication efficiency, antigenicity and neutralization sensitivity of SHIV.C.CH505.375H derived from the first generation design scheme (GenBank accession no. KU958487) and the second generation design scheme (GenBank accession no. MW410742). Equal proportions of SHIV.CH505.375H version 1, version 2, and an "intermediate version" where only the 5' *tat* redundancy was eliminated, were inoculated intravenously into two RMs. Replication kinetics were determined by plasma vRNA quantification (**A**) and relative proportions of the three variants were determined by single genome sequencing (**B**). Neutralization of version 1 and 2 SHIVs by prototypic human bNAb mAbs, the CD4-induced bridging sheet targeted mAb 17b, and polyclonal anti-HIV-1 IgG (HIVIG-C) and serum (CH1754) is depicted (**C**).

1415 **Figure 6.** Neutralization sensitivity of SHIVs bearing wildtype Env375 residues (black symbols) or
1416 alternate Env375 residues preferred for replication in RMs (Trp – blue, His – green, Tyr –
1417 purple). 293T cell derived virus was assayed for entry into TZMbl cells in the presence or
1418 absence of anti-HIV-1 mAbs, polyclonal human anti-HIV IgG preparations (HIVIG-B, -C), or
1419 plasma from a human subject CH1754 chronically infected by HIV-1 (103). The x-axis depicts
1420 antibody concentration (μg/ml) except for CH1754 plasma, which is depicted as a percentage
1421 dilution.

1422 **Figure 7.** Inhibition of SHIV entry into TZMbl cells by the selective CCR5 and CXCR4 coreceptor
1423 inhibitors Maraviroc and AMD-3100, respectively. HIV-1 YU2 Env utilizes CCR5 exclusively for
1424 cell entry and HIV-1 SG3 Env utilizes CXCR4 exclusively, as shown. Entry of the ten SHIVs bearing
1425 wildtype or rhesus-preferred Env375 alleles was inhibited >99% by Maraviroc but minimally or
1426 not at all by AMD-3100, indicating dependence on CCR5 for cell entry.

1427 **Figure 8.** (**A**) Pixel plots (https://www.hiv.lanl.gov/content/sequence/pixel/pixel.html) of single
1428 genome sequences of 3' half genomes of rhesus CD4+ T cell grown SHIV challenge stocks. Tic
1429 marks indicate nucleotide differences from the SHIV molecular clones (T – red, G – yellow, C –
1430 blue, A – green, APOBEC site – green+pink, INDELs – grey). GenBank accession numbers of the
1431 SHIV challenge stock sequences are MW508063 - MW508110 (SHIV.C.1086), MW508111 -
1432 MW508159 (SHIV.B.B41), MW508160 - MW508202 (SHIV.C.CH1012), MW508203 - MW508226
1433 (SHIV.D.191859), MW507934 - MW507964 (SHIV.C.CH505.s1), MW507965 - MW508022
1434 (SHIV.C.CH505.s2), MW508023 - MW508062 (SHIV.C.CH848), MW508227 - MW508279
1435 (SHIV.AG.T250-4), MW484951-MW484987 (SHIV.A.BG505.s1), MW507843 - MW507933
1436 (SHIV.A.BG505.s2) and MW508280 - MW508333 (SHIV.C.CE1176). (**B**) Pie diagrams showing

1437 the relative proportions of different Env375 alleles in SHIV.C.CE1176 and SHIV.AG.T250-4
1438 challenge stocks (see text for explanation).

1439 **Figure 9.** Neutralization sensitivity of SHIVs bearing rhesus-preferred Env375 residues and
1440 generated in either 293T cells (black symbols) or primary rhesus $CD4^+$ T cells (red symbols). For
1441 SHIV.C.CH505, the rhesus $CD4^+$ T cell derived stock 1 is depicted by red symbols and stock 2 by
1442 blue symbols.

1443 **Figure 10.** Plasma viral load kinetics following atraumatic penile inoculation of SHIV.D.191859
1444 (**A**) and atraumatic intrarectal inoculation of SHIV.A.BG505.N332.375Y (**B**). Two RMs (RM41 and
1445 RM42) were inoculated atraumatically a single time with 0.25 ml of undiluted SHIV.D.191859
1446 stock into the sulcus between penile glans and foreskin. This resulted in productive clinical
1447 infection in both animals, as indicated by plasma viremia one week later. Plasma viral load
1448 kinetics through 13 weeks of follow-up were comparable to SHIV.D.191859 plasma virus loads
1449 resulting from other routes of transmission where data were reported earlier (35, 101) and
1450 similar to plasma viremia of SHIV.A.BG505.N332.375Y following low-dose intrarectal challenge
1451 (**B**). Of note, none of the nineteen RMs depicted in panels A and B had been treated with anti-
1452 CD8 mAb, thus demonstrating consistent replication kinetics by different SHIVs administered by
1453 different mucosal inoculation routes.

1454

Table 1A. Genetic and biological features of HIV-1 Envs used for new SHIV constructions

HIV-1 Env	Subtype	Env GenBank Accession#	SHIV GenBank Accession#	Env properties	References
Q23.17	A	AF004885	MW410736	Cloned from primary isolate; binds V1V2 bNAb UCAs	39, 52-54
WITO4160	B	FJ496176	MW410737	T/F[#]; binds V1V2 bNAb UCAs	52-54, 73
B41*	B	EU576114	MW410732	T/F; SOSIP immunogen	47, 73
CE1176	C	FJ444437	MW410733	T/F; global neutralization panel	41, 43
CH1012	C	MG898887	MW410734	T/F; elicited bNAbs in human	50
ZM233	C	DQ388517	MW410738	Cloned from primary isolate; binds V1V2 bNAb UCAs	52-54, 64
1086	C	FJ444395	MW410739	T/F; P5 vaccine trial	43-46
CH0694	C	KJ700458	MW410741	T/F; elicited bNAbs in human	50,51
RV217.40100	AE	MN792078	MW410740	T/F; Thai AE subtype	48, 49
T250-4[&]	AG	MW507842	MW410735	Primary isolate; binds V1V2 bNAb UCAs	20, 52-54

Table 1B. Genetic and biological features of HIV-1 Envs used in previous SHIV constructions

HIV-1 Env	Subtype	Env GenBank Accession#	SHIV GenBank Accession#	Env properties	Reference
BG505^	A	DQ208458	KU958484	T/F; elicited bNAbs in human; SOSIP immunogen	55, 56, 61
YU2	B	M93258	KU958489	Macrophage-tropic; brain-derived	57, 58
CH505	C	KC247556	KU958487	T/F; elicited bNAbs in human	59
CH848	C	KX216883	KU958488	T/F; elicited bNAbs in human	60
CAP256SU	C	KF241776	MT509359	T/F; binds V1V2 bNAb UCAs	52-54, 62
191859	D	JX203061	KU958486	T/F; macrophage-tropic	63

[#] T/F denotes transmitted/founder viral genomes, as reported in the references cited.

* B41 Env is also designated as 9032.08_A1 (73).

[&] T250-4 is one of several *env* molecular clones from the isolate CRF_AG_250. One of these clones was designated by Ellenberger and colleagues as "250" and contributed to the NIH HIV Reagent Program (catalog #11594) and to GenBank (accession #EU513189). This "250" *env* clone #EU513189, when expressed in 293T cells and used to pseudotype an *env*-minus HIV-1 proviral backbone, yields non-infectious virions in the TZM-bl assay (G.M.S., unpublished). The T250-4 *env* clone (GenBank accession #MW507842) differs from #EU513189 by six nucleotides and three amino acids and yields highly infectious HIV-1 Env-pseudotyped virions and highly infectious SHIV.T250-4 virions (see Table 2).

^ SHIV.BG505 exists in two versions with and without an asparagine and potential N-linked glycan at Env residue 332 (35).

Table 2. SHIV challenge stocks expanded in primary rhesus CD4$^+$ T cells

Virus Stock	Volume/ vial (ml)	Date generated	Vials	p27 ng/ml	vRNA copies/ml	Infectivity Titer (IU/ml) TZMbl	Infectivity Titer (IU/ml) rhCD4+ T cells	IU/Particle ratio[#]	AID_{50}^
SHIV.BG505.332N.375Y.dCT(s1▪)	0.75	2/24/16	1,567	154	2,105,956,647	13,437,500	630,957	0.0128	1:3*, 1:120▵
				270[$]	2,263,660,000[$]	6,093,000[$]	165,000[$]	0.0054[$]	
SHIV.BG505.332N.375Y.dCT(s2□)	1.0	1/28/19	2,080	365	4,089,870,000	31,640,000	4,050,000	0.0155	
SHIV.CH505.375H.dCT(s1)	0.5	12/22/15	1,194	178	631,771,853	6,797,000	186,209	0.0215	1:2*, 1:80▵
SHIV.CH505.375H.dCT(s2)	1.0	5/10/17	1,626	190	778,255,000	5,234,400	631,000	0.0135	1:80△
SHIV.CH848.375H.dCT	1.0	4/28/16	1,355	73	900,447,863	4,421,000	162,000	0.0098	
SHIV.191859.375M.dCT	0.25	10/21/14	192	212	3,004,673,792	31,898,389	630,957	0.0212	1:3*
SHIV.B41.375H.dCT	1.0	10/27/17	1,675	200	1,710,815,153	8,125,000	369,000	0.0095	
SHIV.1086.375W.dCT	1.0	2/12/18	2,057	207	502,180,000	146,000	1,870	0.0006	
SHIV.CH1012.375Y.dCT	1.0	2/3/20	2,216	552	1,576,865,000	4,687,000	125,000	0.0059	
SHIV.Ce1176.375HFW.dCT[&]	1.0	2/4/20	2,224	390	1,619,830,000	6,562,000	125,000	0.0081	
SHIV.T250-4.375HWY.dCT[%]	1.0	2/14/20	1,231	634	1,939,331,667	7,656,000	125,000	0.0079	1:160▵+

[#] IU/particle ratio determined on TZMbl cells assuming two vRNA molecules/virion

^ AID_{50} - Inoculum dose leading to productive clinical infection in 50% of rhesus macaques

* Intravaginal (IVAG) inoculation route (1 ml of 1:X dilution)

▵ Intrarectal (IR) inoculation route (1 ml of 1:X dilution)

▪ First stock expansion

□ Second stock expansion

[$] Repeat measurements performed on samples stored for three years in vapor phase liquid nitrogen

[&] Stock comprised of a mixture of Env375 His, Phe and Trp variants

[%] Stock comprised of a mixture of Env375 His, Trp and Tyr variants

[+] Intrarectal AID_{50} estimate of SHIV.T250-4.375HWY.dCT by D Sok and E Rakasz (unpublished)

Table 3. Characteristics of SHIV inocula and clinical outcomes of 41 rhesus macaques

SHIV strain	Sub-type	Wildtype 375 residue	Animal ID	375 variant	Number of variants	Stock derivation	Dosage P27 ng*	Route[Δ]	CD8 Depletion	Peak VL[$]	Setpoint VL	Preferred 375 residues[#]	Clinical AIDS
CE1176	C	375-Ser	6445	S, M, H, Y, F, W	6	293T	300	IV	No	673,106	1,016	H, W	No
			6448	S, M, H, Y, F, W	6	293T	300	IV	No	482,934	<250	W, H	No
			6562	S, M, H, Y, F, W	6	293T	300	IV	No	29,252	<250	W, F	No
			6563	S, M, H, Y, F, W	6	293T	300	IV	No	894,432	20,608	F, W	No
CH1012	C	375-Ser	T679	S, M, H, Y, F, W	6	293T	300	IV	No	4,814,098	<250	Y, W, H	No
			T680	S, M, H, Y, F, W	6	293T	300	IV	No	4,759,788	<250	Y, W	No
			6928	Y	6	293T	50	IV	Yes	42,350,830	8,830		No
			6929	Y	6	293T	50	IV	Yes	25,654,060	39,992		Yes
			6930	Y	6	293T	50	IV	Yes	14,495,480	10,656		Yes
T250-4	AG	375-Ser	6709	S, M, H, Y, F, W	6	293T	300	IV	No	471,828	<250	H, W	No
			6716	S, M, H, Y, F, W	6	293T	300	IV	No	1,744,646	5,708	W, Y, F	No
			40701	S, M, H, Y, F, W	6	293T	300	IV	No	932,684	0	W, H	No
			6925	Y, H, W, F	1	293T	200	IV	Yes	67,161,230	8,900	H	No
			6926	Y, H, W, F	1	293T	200	IV	Yes	9,600,904	29,196	H	Yes
			6927	Y, H, W, F	1	293T	200	IV	Yes	42,558,680	23,966	H	No
Q23.17	A	375-Ser	41298	S, M, H, Y, F, W	6	293T	300	IV	No	122,560	<250	H, Y, F, W	No
			41852	S, M, H, Y, F, W	6	293T	300	IV	No	173,420	7,680	H, Y, F, W	No
			T280	H	1	293T	50	IV	Yes	29,118,930	29,000,000		Yes
WITO4160	B	375-Thr	40651	T, S, M, H, Y, F, W	7	293T	350	IV	No	1,222,790	1,922	W, Y	No
			40723	T, S, M, H, Y, F, W	7	293T	350	IV	No	2,226,030	8,564	W, Y	No
			40863	T, S, M, H, Y, F, W	7	293T	350	IV	No	3,044,620	1,648	W, Y	No
ZM233	C	375-Ser	41412	S, M, H, Y, F, W	6	293T	300	IV	No	51,052	<250	F, H, Y	No
			41537	S, M, H, Y, F, W	6	293T	300	IV	No	408,840	2,390	Y, H, F	No
			41712	S, M, H, Y, F, W	6	293T	300	IV	No	364,598	7,068	Y, F, H, M	No
			40717	Y	1	293T	50	IV	Yes	1,432,284	18,936		No
			11D042	Y	1	293T	50	IV	Yes	61,300,980	88		No
			K12	Y	1	293T	50	IV	Yes	4,445,834	2,072		No
1086	C	375-Ser	T682	S, M, H, Y, F, W	6	293T	300	IV	No	190,208	11,062	W	Yes
			T683	S, M, H, Y, F, W	6	293T	300	IV	No	682,242	2,090	W, Y	No
			T684	S, M, H, Y, F, W	6	293T	300	IV	No	3,144,292	<250	W	No
			T929	W	1	293T	50	IV	Yes	2,679,424	20,138		No
			T930	W	1	293T	50	IV	Yes	2,648,942	7,944		No
CH0694	C	375-Thr	T931	T, S, M, H, Y, F, W	7	293T	350	IV	Yes	7,778,446	106,716	Y	No
			T932	T, S, M, H, Y, F, W	7	293T	350	IV	Yes	472,192	2,928	Y, F	No
			T933	T, S, M, H, Y, F, W	7	293T	350	IV	Yes	3,718,208	119,506	Y	No
B41	B	375-Ser	41949	S, M, H, Y, F, W	6	293T	300	IV	No	11,980,270	285,856	H, W, Y	No
			42534	S, M, H, Y, F, W	6	293T	300	IV	No	16,044,860	24,314	H, W	No
			42579	S, M, H, Y, F, W	6	293T	300	IV	No	4,332,634	387,742	H,W	Yes
RV217.40100	AE	375-His	40973	S, M, H, Y, F, W	6	293T	300	IV	No	370,894	0	W	No
			41193	S, M, H, Y, F, W	6	293T	300	IV	No	81,162	0	W	No
			41216	S, M, H, Y, F, W	6	293T	300	IV	No	1,555,258	3,380	W	No

* Inocula consisted of 50 ng p27Ag equivalent of each Env375 SHIV variant

[Δ] IV – intravenous bolus by slow push

[$] VL – virus load (vRNA molecules/milliliter of plasma)

[#] Preferred Env375 allelic variants in plasma (H-His, W-Trp, F-Phe, Y-Tyr, M-Met)

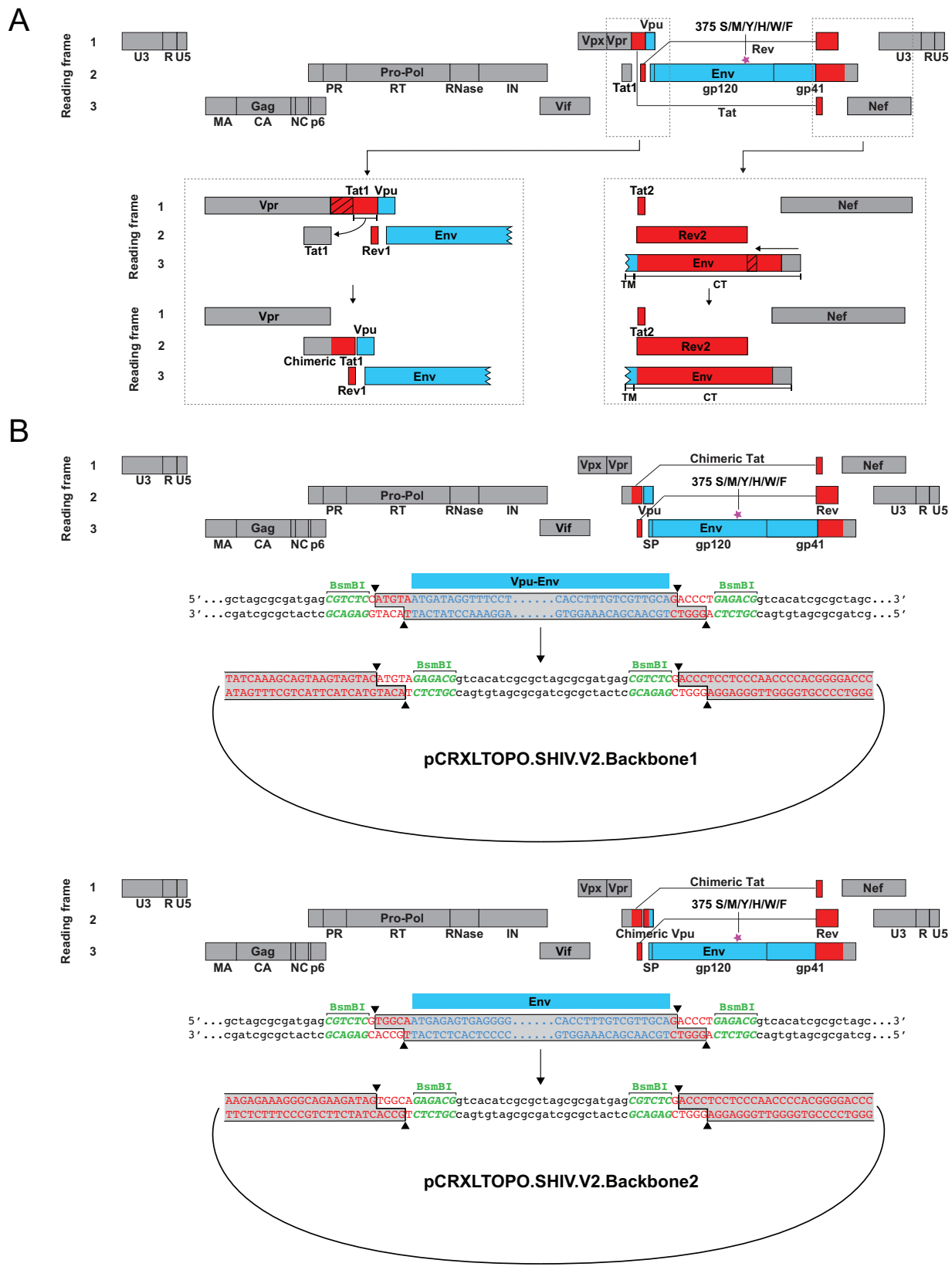

Figure 1

Black: linker/adaptor sequences
Green: BsmBI recognition site
Red: Backbone sequence
Blue: Vpu/Env or Env of interest

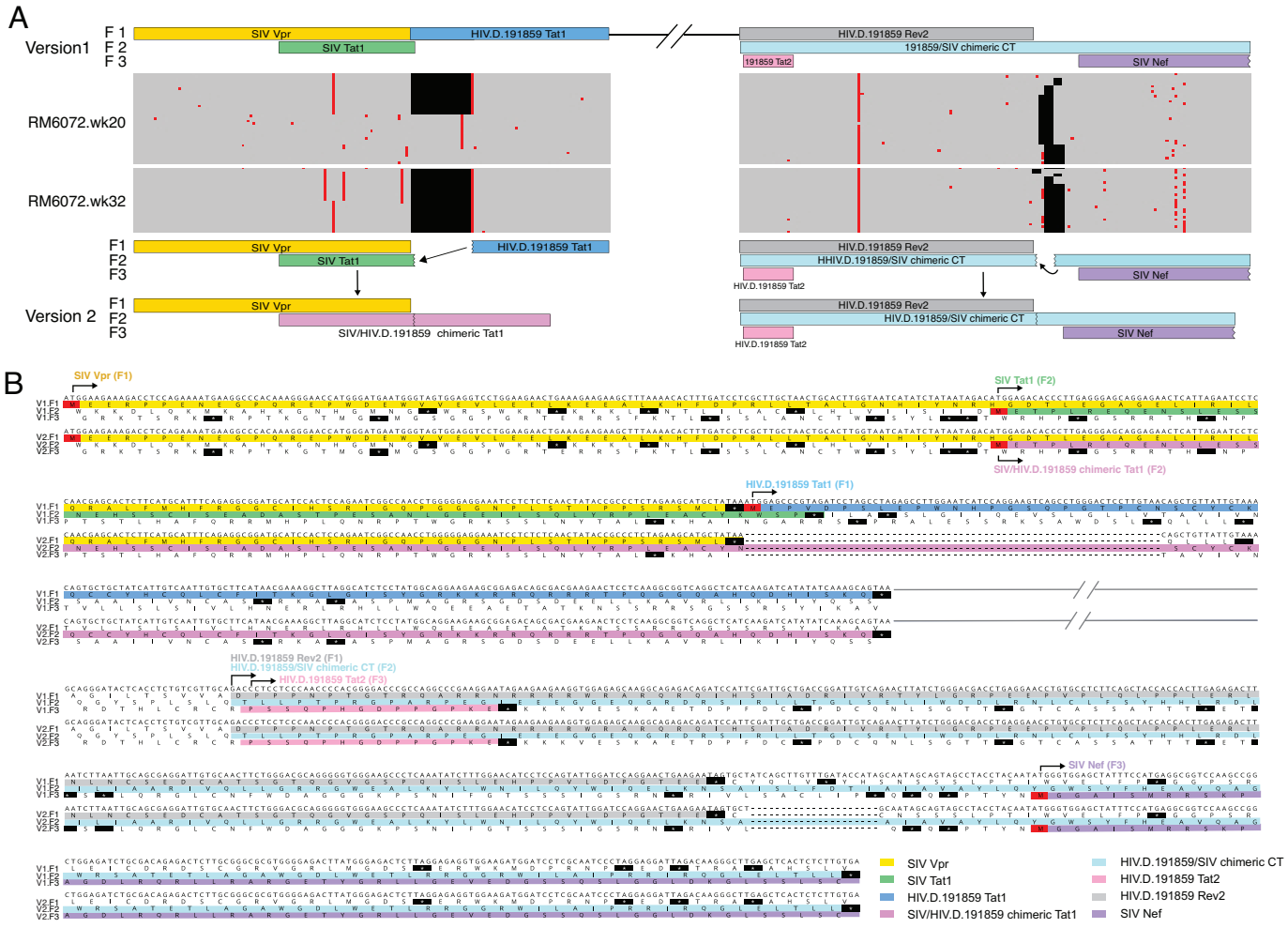

Figure 2

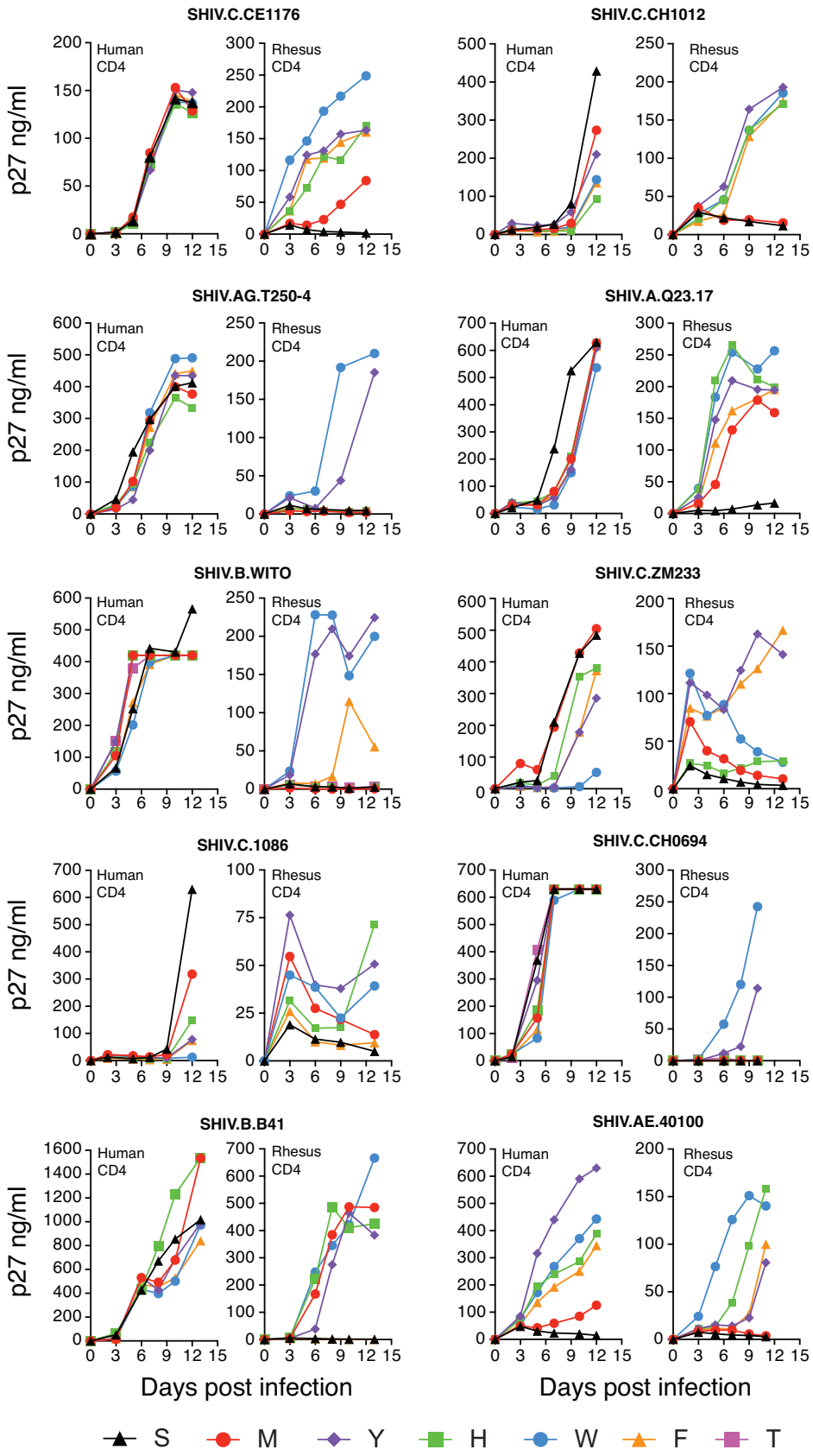

Figure 3

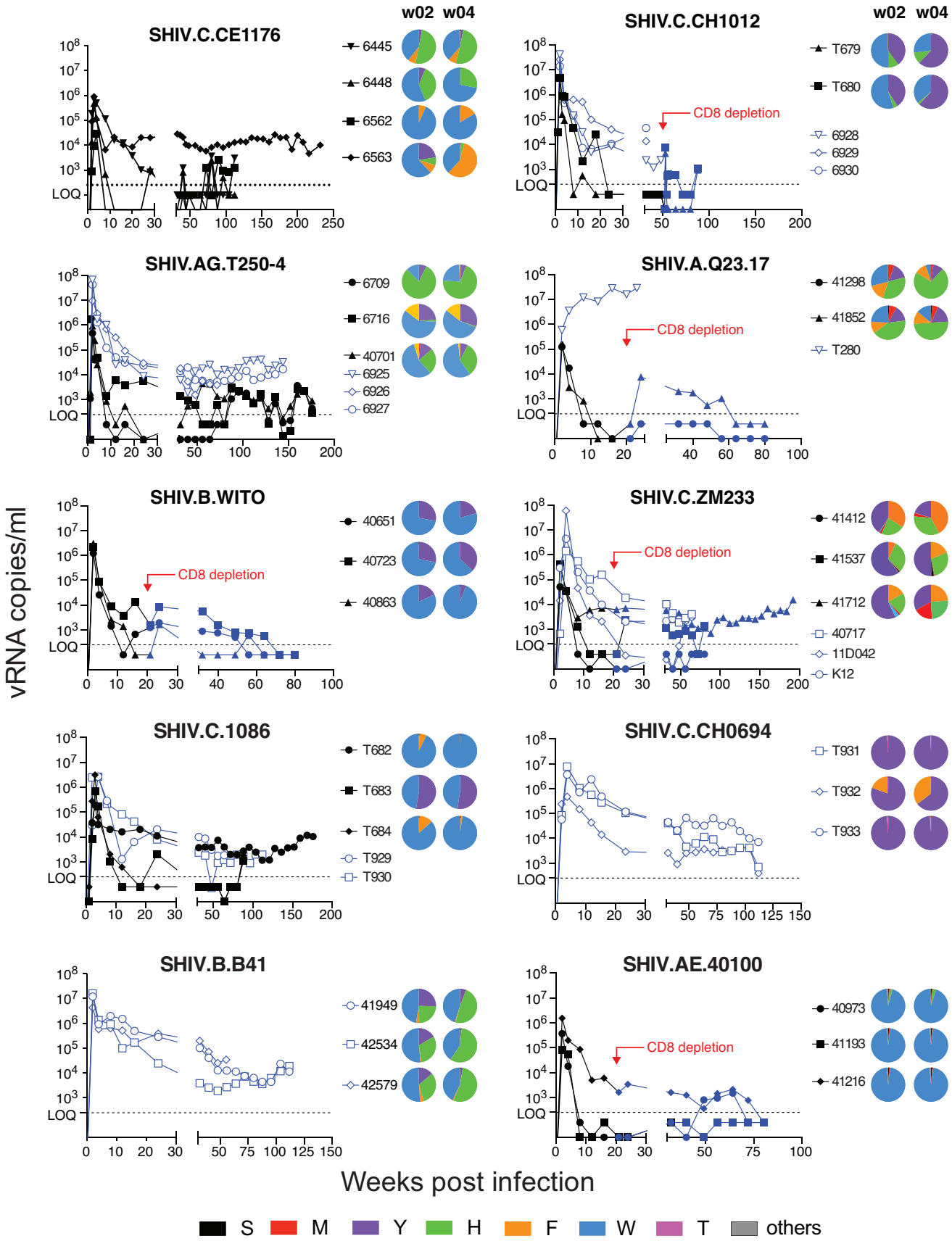

Figure 4

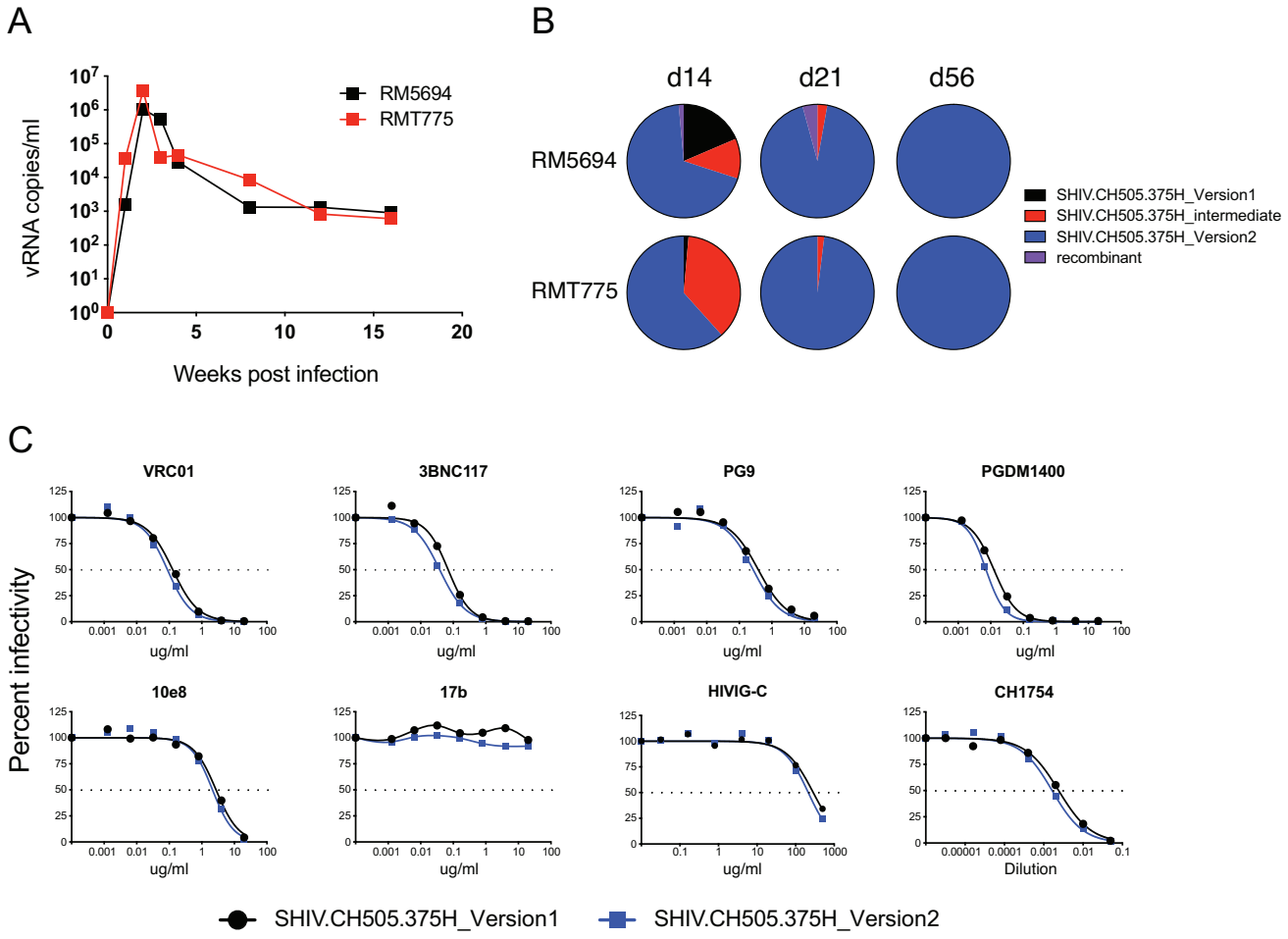

Figure 5

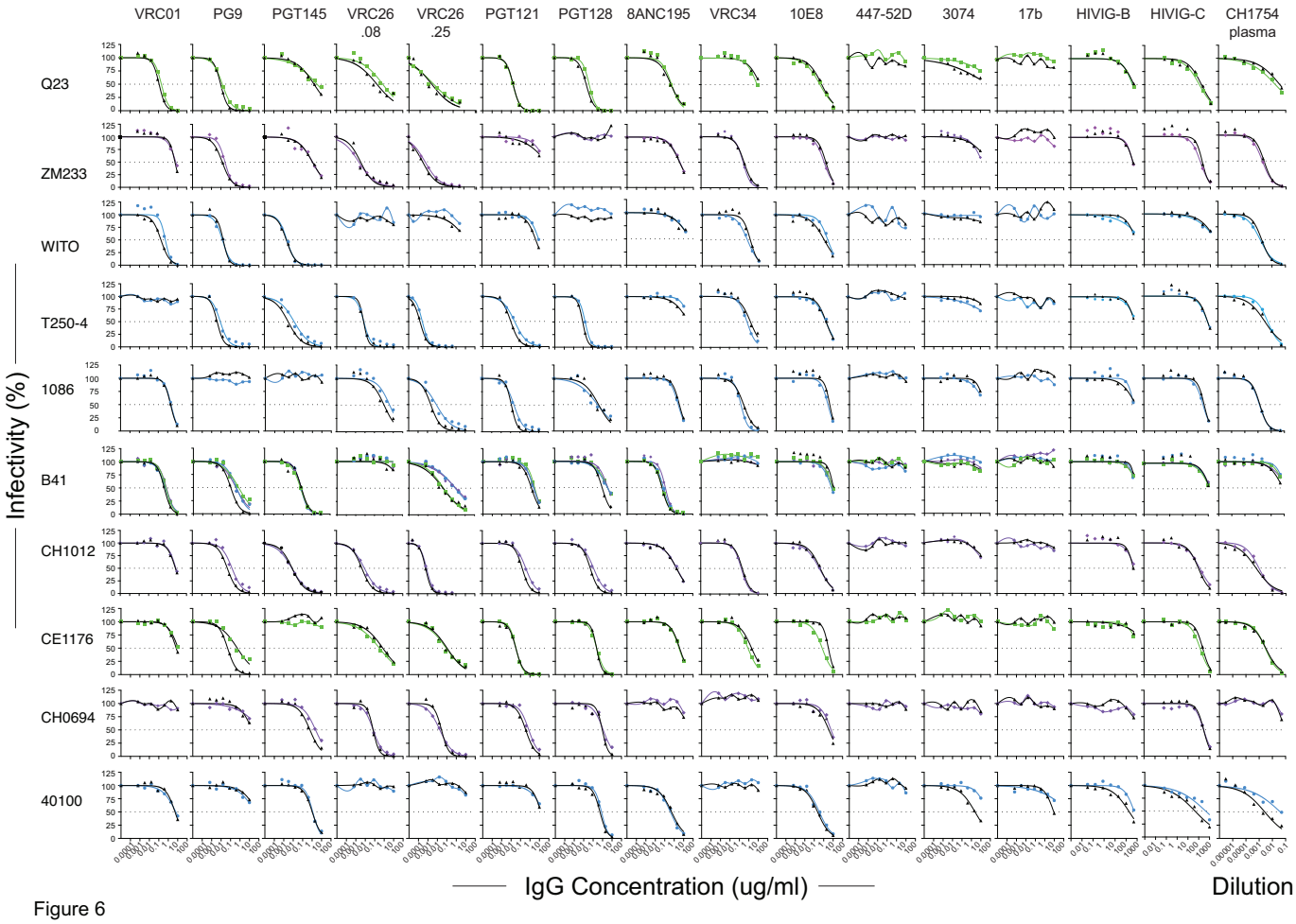

Figure 6

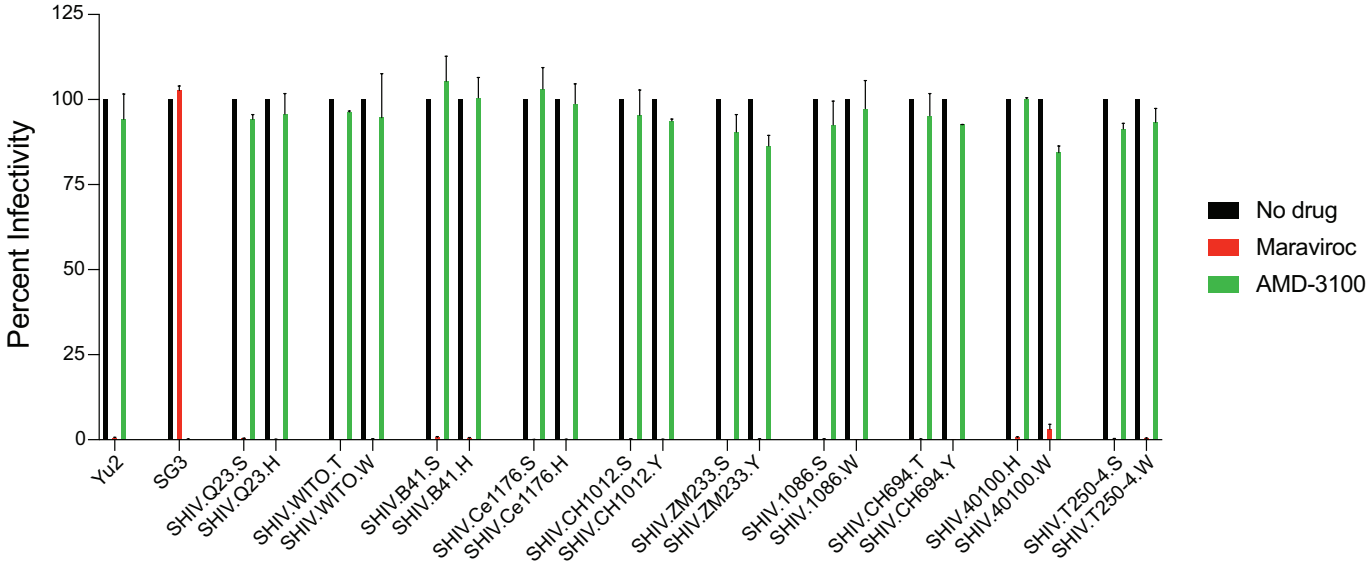

Figure 7

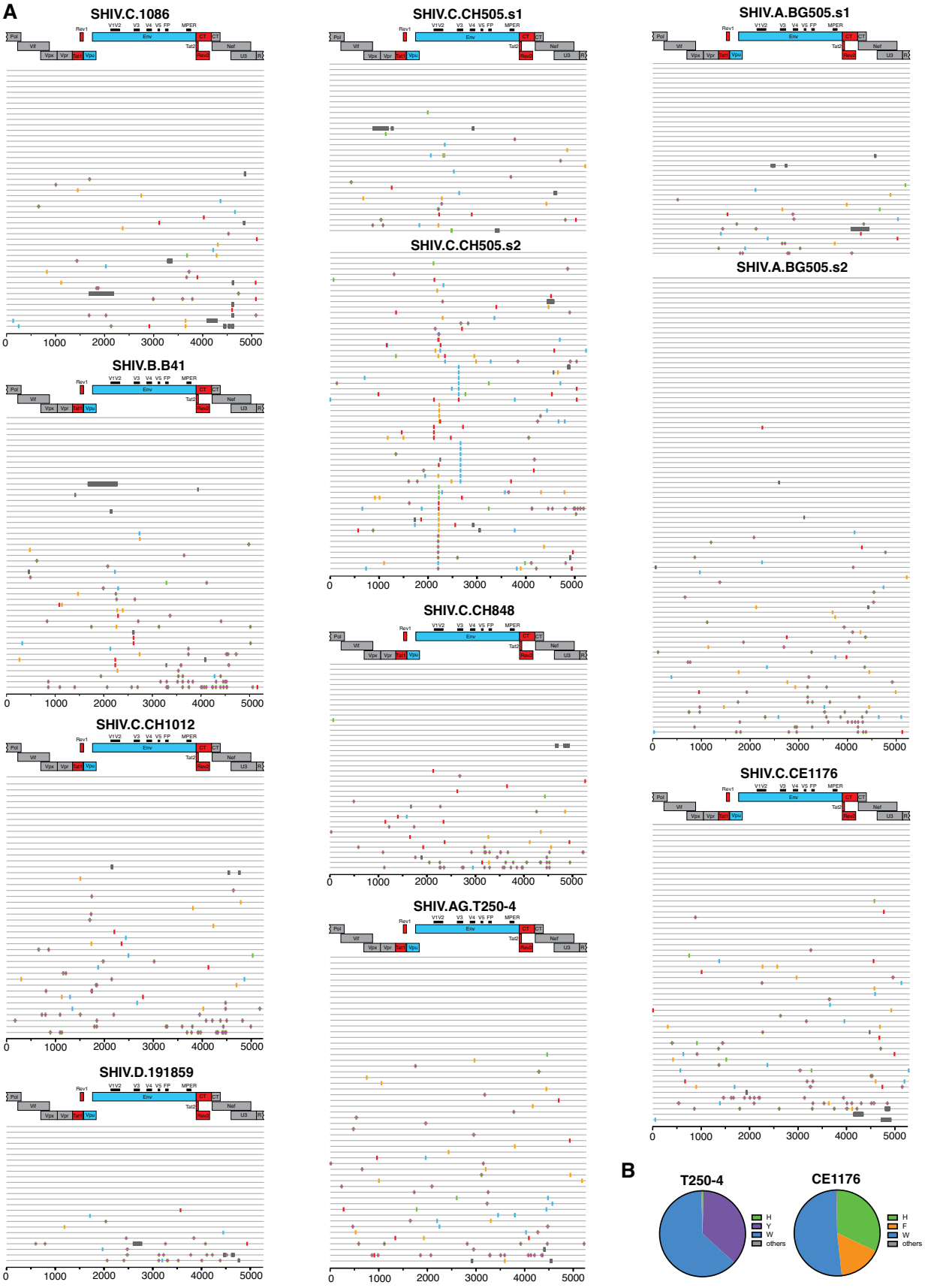

Figure 8

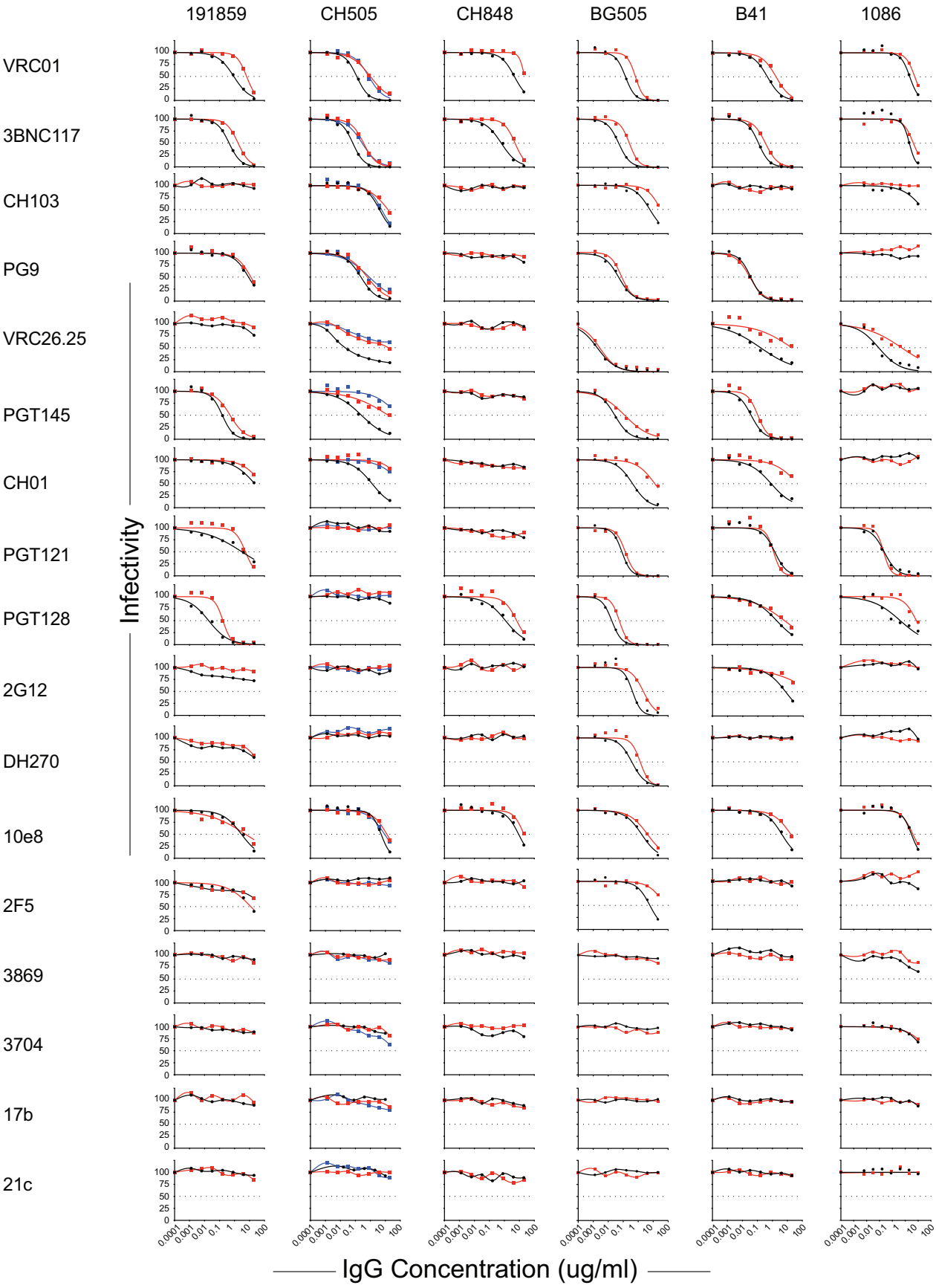

Figure 9

Journal of Virology
JVI
Journal of Virology

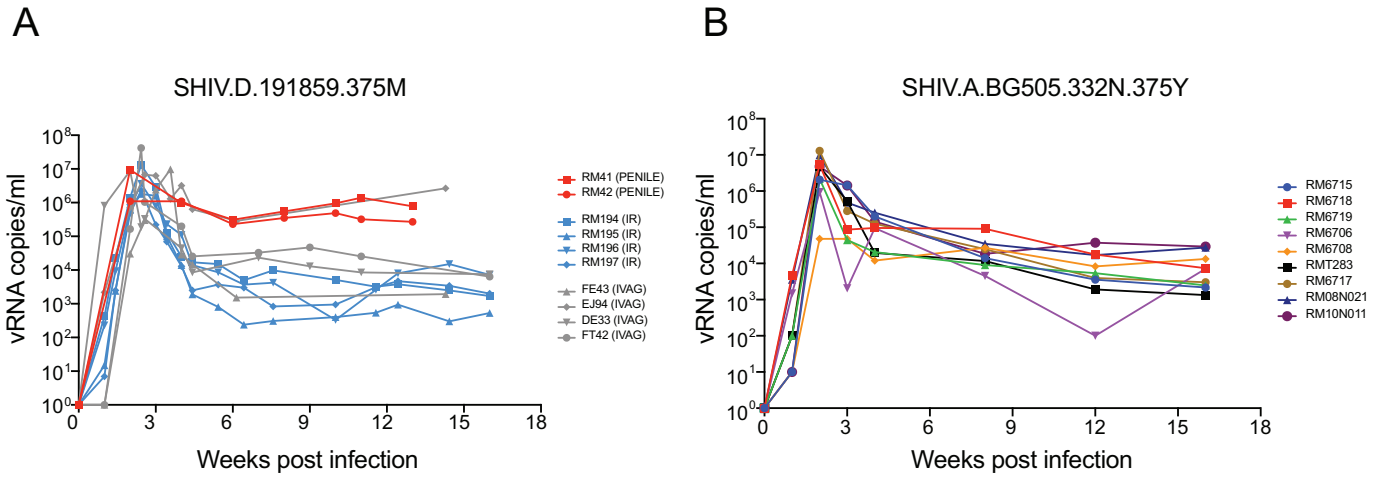

Figure 10